The Tom1L1-clathrin heavy chain complex regulates membrane partitioning of the tyrosine kinase Src required for mitogenic and transforming activities.

Guillaume Collin, Mélanie Franco, Valérie Simon, Christine Bénistant, Serge Roche

The Tom1L1-Clathrin Heavy Chain complex regulates membrane partitioning of the tyrosine kinase Src required for mitogenic and transforming activities

Guillaume Collin[1,3], Mélanie Franco[1,2,3], Valérie Simon[1], Christine Bénistant[1] & Serge Roche[1*]

[1]CNRS UMR5237 University of Montpellier 1 and 2, CRBM, 1919 route de Mende, 34293 Montpellier, France

[*]**Correspondence**: Serge Roche

34293 Montpellier Cedex 05, France.

Tel: +33 467 61 33 73

Fax: 33 467 52 15 59.

Email: Serge.Roche@crbm.cnrs.fr

Running title: Regulation of Src signaling by Tom1L1-CHC

Words count: 7828

Materials and Methods: 850

Introduction, Results, Discussion: 3746

[2]current address: Division of Molecular Oncology, IRCC University of Torino School of Medicine, 10060 Candiolo, Turin, Italy.

[3]Equal contribution to the manuscript

ABSTRACT

Compartmentalization of Src tyrosine kinases (SFK) plays an important role for signal transduction induced by a number of extracellular stimuli. For example, Src mitogenic signaling induced by the growth factor Platelet-Derived Growth Factor (PDGF) is initiated in cholesterol-enriched microdomains caveolae. How this Src sub-cellular localization is regulated is largely unknown. Here we show that the Tom1L1-Clathrin Heavy Chain (CHC) complex negatively regulates the level of SFK in caveolae needed for the induction of DNA synthesis. Tom1L1 is both an interactor and a substrate of SFK. Intriguingly, it stimulates Src activity without promoting mitogenic signaling. We found that, upon association with CHC, Tom1L1 reduced the level of SFK in caveolae, thereby preventing its association with the PDGF receptor, which is required for the induction of mitogenesis. Similarly, the Tom1L1-CHC complex reduced also the level of oncogenic Src in cholesterol-enriched microdomains, thus affecting both its capacity to induce DNA synthesis and cell transformation. Conversely, Tom1L1, when not associated with CHC, accumulated in caveolae and promoted Src-driven DNA synthesis. We concluded that the Tom1L1-CHC complex defines a novel mechanism involved in negative regulation of mitogenic and transforming signals, by modulating SFK partitioning at the plasma membrane.

INTRODUCTION

The cytoplasmic tyrosine kinases of the Src family (SFK) play important roles in signal transduction induced by growth factors leading to DNA synthesis, cytoskeletal rearrangement and receptor endocytosis (5). How growth factors use SFK for transmitting these signals is largely unknown. Signal specificity may be dictated by phosphorylation of appropriate substrates. Additionally, it may be achieved spatially through recruitment of a specific pool of SFK within the cell. Indeed, Platelet-Derived Growth Factor (PDGF)-induced DNA synthesis requires SFK activation in the cholesterol-enriched domains, the caveolae, while cytoskeleton rearrangement requires SFK association with F-actin assembly for dorsal ruffle formation (27). Accordingly, these pools are regulated by distinct mechanisms: mitogenic activity involves direct association of SFK with the receptor in caveolae, while SFK-induced F-actin assembly is mediated by the lipid second messenger sphingosine 1 phosphate. This lipid is likely to promote kinase activation via binding to a heterotrimeric Gi protein-coupled receptor. Therefore, regulation of SFK sub-cellular localization may be an important feature of signaling specificity. The molecular mechanism that governs such a compartmentalization is an important issue that remains yet unexplained.

Cholesterol-enriched microdomains are membrane organelles with specific physical features that are distinct from the contiguous membrane (26). While subjected to intense debates, they are thought to function as lipid scaffolds to regulate signal transduction induced by a number of extracellular stimuli including T cell receptor complexes (6, 18). Caveolae define a subclass of these membrane structures in non-lymphoid cells with a diameter of 50-100 nm and represent the major cholesterol-enriched microdomains present in fibroblasts. They are composed of caveolins, the main structural proteins, cholesterol and sphingolipids, and a number of signaling molecules including growth factor receptors and SFK. Compelling

evidences indicate that they regulate signal transduction induced by growth factors and integrins in non-transformed cells (19).

Src is subjected to strict control in non-transformed cells and constitutive kinase activation leads to oncogenic properties (17). Catalytic regulation involves intramolecular interactions (e.g. SH2 with the phosphorylated Tyr527 tail and the SH3 with a linker between the SH2 and the catalytic core) that stabilize the kinase in a close and inactive conformation. Opening the conformation by various means is predicted to stimulate the catalytic activity. Moreover, most SrcSH2 and/or SH3 binders increase Src activity in vivo and exhibit mitogenic and/or transforming activity (2). Nevertheless we and others have recently identified Tom1L1 as a novel substrate and Src binder that does not induce mitogenic activity while promoting kinase activity in vitro (8, 25). This adaptor belongs to the Tom1 family of proteins and presents a VHS (Vps27, Hrs and STAM) and a GAT (GGA and Tom1) homology domain implicated in the regulation of vesicular trafficking (3, 16), a linker region and a unique C-terminus for phosphorylation and interaction with Src. Here we show that Tom1L1 interacts with Clathrin Heavy Chain (CHC) in vivo, a structural component of clathrin-coated vesicles. Tom1L1, when bound to CHC, negatively regulates Src mitogenic and transforming activities by reducing its level in cholesterol-enriched microdomains including caveolae. Conversely, Tom1L1, when not associated with CHC, relocates in the caveolae and promotes Src-driven DNA synthesis. Therefore, the Tom1L1-CHC complex defines a novel mechanism for regulation of Src mitogenic and transforming activities, by influencing the kinase's membrane partitioning.

MATERIAL AND METHODS

Reagents.

pBABE and pSGT constructs encoding murine Tom1L1, YFPP (Tom1L1 R419D/P421A/P424A/Y457F), ΔL (deletion of amino acids 292-386), ΔL/YFPP, SrcY527F, PDGFRβ and Cav-3DGV were described in (8, 23, 27). ΔC (deletion at amino acid 386 of murine Tom1L1), ΔL/L401A (L401A/L402A/L407A) construct was obtained by PCR using the Quick Change Site-directed Mutagenesis System (Stratagene). Green Fluorescent Protein (GFP)-Tom1L1 constructs were obtained by sub-cloning Tom1L1 into pEGFP. Constructs encoding CHC *Discosoma sp* red (DsRed) (30) and Gst-CHC terminal domain (7) were from P. Coopman and D. Drubin respectively. Control (scramble) and siRNA specific to murine Tom1L1 (8), murine CHC (AACCGCATGGAGACATAATAT) and human CHC (10) were purchased from Qiagen. Mock or shRNA specific to human Tom1L1 was obtained from the pSiren retroviral vector encoding shRNA specific to Luciferase (mock) or shRNA that target the GACAAGAGACTGCTAAAT sequence of human Tom1L1. Polyclonal Tom1L1.1-3 antibodies were raised against GST-fusion proteins containing the full-length (anti-Tom1L1.1), amino acids 291-474 (anti-Tom1L1.2) and amino acids 1-291 (anti-Tom1L1.3) of the murine Tom1L1 and were described in (8). Antibodies specific to Src, Fyn and Yes (cst1), PDGFRβ (PRC), mT (762) myc tag (9E10), tubulin and 4G10 have been described in (4, 8, 27). αCHC used for immunoprecipitation (X22) and for Western blotting (TD.1) were from Alexis Biochemicals and Sigma respectively; anti-pan-caveolin from Transduction Laboratory, EC10 (anti-avian Src) from UBI, antibodies coupled to fluorescent probes from Molecular Probe, BrdU from Sigma, anti-BrdU from Pharmingen, PDGF-BB from AbCys and SU6656 from Calbiochem. Purified Gst fusion proteins and SFK were described in (8).

Cells culture, transfection, retroviral infection, immunofluorescence, DNA synthesis and cell transformation

NIH 3T3, SrcY527F-NIH 3T3 (Src 527), HEK 293 and HeLa cells were cultured as described in (1, 8). HEK 293 cells stably expressing PDGFRβ were obtained followed by infection of retroviruses expressing the human receptor (gift of A. Kazlauskas, Harvard Medical School, Boston USA). Transfection and retroviral infection procedures were described in (4, 13). Cell transformation assays were performed using NIH 3T3 cells infected with indicated retroviruses, transfected or not with the indicated siRNA using Lipofect-AMINE reagent (Invitrogen) and maintained in 10% FCS for 10-12 days. After staining with crystal violet (1%), the number of foci was visually scored. For BrdU incorporation assays, NIH 3T3 cells were seeded onto coverslips and made quiescent by serum starvation for 30 h. Cells were next stimulated or not with PDGF (5 - 20 ng/ml) in the presence of BrdU (0.1 mM) for 18 h. When indicated cells were treated with SU6656 (2 μM) 30 min before stimulation and/or BrdU addition. Cells were then fixed and processed for immunofluorescence as described in (9). The % of transfected cells, which incorporated BrdU for each coverslips, was calculated using the following formula: % BrdU-positive cells = [number of BrdU-positive transfected cells] / [number of transfected cells] × 100. For siRNA experiments, cells were transfected and serum starvation was started 48 h afterwards. Caveolae immunostaining was performed using anti-pan caveolin on cells fixed with ice cold methanol, which allows detection of caveolin present in mature caveolae (20). Src (or Tom1L1)/caveolin co-localization at the cell periphery was detected by confocal analysis of 20-30 cells for each experiment and calculated as follows % = {number of transfected cells that exhibit co-localization at the cell periphery} / {number of transfected cells} × 100. Cells were observed with a Carl Zeiss LSM510 META confocal microscope and a 100X PL APO (NA=1.4) oil immersion objective. Confocal images were acquired using the single track mode and Ar 488nm and HeNe 543nm excitation. FITC and rhodamine channels were acquired using a BP 505/530 filter and a custom 550-603 filter (ChS) respectively. For CHC co-localization, cells were fixed with 3.7% formaldehyde before

immunostaining. Fixed cells were observed with a DMRB oil immersion microscope APO 63X (Leica). Acquisition was performed with a cooled CCD Micromax camera (Princeton Instruments) driven by MetaMorph 6.2 (Molecular Device). Stacks of images were restored using Huygens 2.3 (Scientific Volume Imaging) and a MLE algorithm.

Biochemistry.

Cell-lysates, pull-down assays, immunoprecipitation, Western blotting, kinase assays and re-immunoprecipitations were performed as described in (8, 27). For biochemical analysis, cells were stimulated 1 h on ice with PDGF (25 ng/ml) as described in (22). Fractionation experiments were performed essentially as described in (27). Briefly, scrapped cells were centrifuged and pellets suspended in 2 X-Lysis Buffer containing 1% Triton X-100, 10 mM Tris-HCl (pH 7.5), 150 mM NaCl, 5 mM EDTA, 75 units/ml aprotinin and 1 mM vanadate, for 20 min. Cell suspensions were homogenized with a Dounce homogenizer and centrifuged to remove nuclei. Supernatants were subjected to (5 - 42.5%, w/v) sucrose gradient centrifugation and 9 fractions were collected from the top to the bottom of each gradient. CEF corresponded to collected fractions 2-4 and were treated as in (27) before biochemical analysis. Purification of Gst fusion proteins and Gst cleavage were performed as described in (8). Tyrosine phosphorylated Tom1L1 proteins were generated as follows: after excision of the Gst sequence, proteins were phosphorylated in vitro by incubation with Gst-FynSH1 bound to glutathione beads with 0.1 mM ATP for 30 min at 30°C. ATP was then removed from the supernatant using G-50 minicolumns (Amersham).

RESULTS

CHC-Tom1L1 complex formation.

The negative mitogenic regulation of Tom1L1 requires its C-terminus and the linker regions (8). We then searched for interactors involved in this activity through an affinity-purification strategy coupled to mass spectrometry using HeLa cell-lysates. CHC was found to be the main interactor of Tom1L1 (VS and SR, unpublished observations) and it was also recently reported by Katoh et al (12). CHC association with GST-Tom1L1 was confirmed by Western blotting using CHC specific antibody (Fig. 1B). The formation of endogenous Tom1L1-CHC complex was suggested by co-immunoprecipitation of CHC with Tom1L1 in NIH 3T3 cells (Fig. 1C). The molecular mechanism by which CHC associates with Tom1L1 was next addressed. First, CHC exhibited in vitro affinity for the VHS, the linker and the C-terminus regions of Tom1L1 (Fig. 1B). The involvement of both the Linker and the C-terminus regions for CHC association were further investigated in vivo. Deletion of either domain reduced the association of Tom1L1 with CHC-DsRed that were co-expressed in HEK 293 cells (Fig. 2A). Mutations in Tom1L1 binding sites for the Src SH2 (Y457) and SH3 domains (P420PLP) had however no effect, indicating that SFK are not involved in this process (mutants YPP and ΔL/YPP in Fig. 2A). Most clathrin partners bind to its N-terminus via Leu motifs called "clathrin boxes" (14). We found that a similar mechanism regulates CHC-Tom1L1 complex formation: the N-terminal domain of CHC fused to Gst (Gst-CHC-TD) associated with Tom1L1 in vitro (Fig. 2B). Moreover, three potential "clathrin boxes" were found in the C-terminus and mutation of the first Leu-rich motif L_{401}LQPVSL into AAQPVSA strongly affected the interaction of Gst Tom1L1 C-terminus (Gst-Cter) with CHC in vitro (Fig 2C; mutant Gst-Cter/L401A). Finally we investigated the importance of the Linker and the L_{401}LQPVSL sequences in Tom1L1-CHC interaction in vivo. The Tom1L1 ΔL/L401 mutant that was deleted from the Linker sequence and where Leu401, Leu402 and Leu407 were replaced by Ala barely associated with endogenous CHC when expressed in HEK 293 cells (Fig. 2D). Moreover, while GFP-Tom1L1 and CHC-DsRed exhibited a strong

co-localization when co-expressed in NIH 3T3 cells, (see Fig. 2E, upper panels), GFP-Tom1L1 ΔL/L401mutant did not co-localize with CHC-DsRed (Fig. 2E, lower panels). We, thus, concluded that the linker and the Leu-rich motif L_{401}LQPVSL present in the C-terminus are required for association of Tom1L1 with CHC.

CHC-Tom1L1-Src complex formation.

Since Tom1L1 binds also to Src, we sought for a CHC-Tom1L1-Src ternary complex formation in vitro. Purified Tom1L1 associated with bound Gst-CHC-TD at a ratio of about 1:1 (Fig. 3A, Brillant Blue Staining), confirming the strong interaction between Tom1L1 and CHC. While no interaction was detected when only Gst-CHC-TD and Src were used in vitro, an association was clearly observed in the presence of Tom1L1 (Fig. 3A). This suggests that Tom1L1 can bridge Src to CHC. Indeed, the association between Src and CHC was barely detected in the presence of Tom1L1/YPP that harbors reduced affinity for Src (8), but retains its strong interaction with Gst-CHC-TD (Fig. 3A). We then addressed the impact of Tom1L1 phosphorylation on the ternary complex formation. pY-Tom1L1, that has been phosphorylated by the catalytic domain of Fyn, was purified in a free form (8) and incubated with bound Gst-CHC-TD for complex formation. As shown in Fig. 3A (bottom panel), Fyn phosphorylation did not affect the capacity of Tom1L1 to interact with Gst-CHC-TD but induced a 4.8 fold increase in Src association with the heterodimer. Src binding was however reduced by two fold when we used the Tom1L1/YPP mutant that exhibited lower tyrosine phosphorylation content (i.e. pY-Tom1L1/YPP) and lower affinity to Src. This data indicates that tyrosine phosphorylation of Tom1L1 regulates association of Src with the Tom1L1-CHC complex.

The interaction of SFK with CHC-Tom1L1 was next evaluated in vivo using HEK 293 cells co-expressing Src and/or Tom1L1 (Fig. 3B). CHC was detected in SFK

immunoprecipitates from cells expressing endogenous level of Tom1L1. Nevertheless, co-immunoprecipitation was significantly enhanced by Tom1L1 overexpression. In contrast CHC-Tom1L1 complex formation was not affected by Src co-expression. It should be mentioned that similar lower levels of SFK and Tom1L1 were detected in CHC immunoprecipitates - lower levels obtained may be due to low efficacy of antibodies to precipitate native clathrin (MF and SR, unpublished observations) -. Accordingly, a role for endogenous Tom1L1 in CHC-SFK interaction was also suggested in NIH 3T3 cells: CHC was detected in SFK immunoprecipitates and its level was reduced by Tom1L1 depletion (Fig. 3C). Finally, imunofluorescence analysis using cells co-expressing Src, CHC-DsRed and GFP-Tom1L1 showed that all three components co-localized in fibroblasts (Fig. 3D). Triple co-localization was observed especially in clathrin-coated vesicles and at the plasma membrane. We concluded that Tom1L1 participates in Src-CHC association.

CHC has been reported as a Src substrate (29), therefore we also investigated the role of Tom1L1 in CHC tyrosine phosphorylation. CHC-TD alone was not phosphorylated by Src in vitro, even in the presence of higher concentrations of the protein (Fig. 3E, left panel). Nevertheless, in vitro phosphorylation was readily detected in the presence of Gst-Tom1L1. This effect was not restricted to Src as similar results were obtained with the tyrosine kinase Fyn (Fig. 3E, right panel). It should be mentioned that in these conditions, Src and Fyn preferentially phosphorylated CHC-TD, suggesting that the association with Tom1L1 allows unmasking of CHC phosphorylation sites. The Tom1L1 role in CHC tyrosine phosphorylation was next investigated in vivo. Co-expression experiments in HEK 293 cells suggested that Src-induced CHC phosphorylation was favored by the presence of overexpressed Tom1L1 (Fig. 3B, left panels). Indeed, we found that endogenous CHC tyrosine phosphorylation was enhanced in NIH 3T3 cells stably expressing oncogenic SrcY527F and this was abrogated by

Tom1L1 depletion (Fig. 3F). We concluded that Tom1L1 additionally regulates Src-induced CHC tyrosine phosphorylation.

The CHC-Tom1L1 complex affects SFK level in caveolae.

We next investigated whether TomL1-CHC affects SFK sub-cellular localization in caveolae. This was first addressed biochemically using caveolae-enriched fractions (CEF) purified from HEK 293 cells expressing Src together or not with Tom1L1. Triton X-100 cell-lysates were homogenized to increase protein solubility and fractionated through a sucrose gradient. CEF were isolated in the light fractions (2-4) as shown by the bulk of caveolin (Fig. 4A) (see also 27). We found that Tom1L1 overexpression strongly reduced the level of SFK in CEF without affecting caveolin accumulation. This inhibition was due to kinase de-localization as Tom1L1 did not affect the whole SFK. Quantification of these experiments indicated that about 50% of SFK was excluded from the CEF (Fig. 4B). In contrast, Tom1L1 did not influence the PDGF receptor (PDGFR) level in these fractions (Fig. 4A and B). This finding indicates that Tom1L1 is not a general regulator of tyrosine kinases partitioning at the plasma membrane. We next investigated the role of CHC on Tom1L1 regulation of SFK level at the CEF. As shown in Fig. 4A and B, down-regulation of CHC by a specific siRNA, strongly reduced the capacity of Tom1L1 to deplete SFK from CEF. Similarly, the reduction of SFK level was not observed with the ΔL/L401A Tom1L1 mutant that can not associate with CHC (Fig. 4A and B). This mutant still retains some capacity to bind Src (8), indicating that the absence of effects on the SFK level was not due to its inability to associate with SFK. Finally, we investigated whether a similar mechanism occurs with endogeneous Tom1L1 (Fig. 4C). Accordingly, down-regulation of Tom1L1 level by 80 % induced a two fold accumulation of endogenous SFK at the CEF, concomitant with a significant reduction of

SFK level in soluble fractions (fractions 7-9). Thus, we concluded that the reduction of SFK level in caveolae is dependent on the association of Tom1L1 with CHC.

The role of Tom1L1-CHC complex on SFK membrane partitioning was next confirmed by an immunofluorescence approach. Src, together or not with Tom1L1, was expressed in fibroblasts by retroviral infection in order to get moderate level of ectopic protein and to prevent aberrant sub-cellular localization. We immunostained caveolae with an antibody, that recognized the caveolin present in these membrane domains, and detected its expression in restricted area of the plasma membrane (Fig. 4D), as previously reported (20). An anti-Src was used to analyze the impact of Tom1L1 expression on Src distribution. An example of such experiments is shown in Fig. 4D and the statistical analysis in Fig. 4E. About 70% of infected cells exhibited a Src/caveolin co-localization at the cell periphery. While Tom1L1 over-expression did not affect membrane caveolin distribution, it induced a two fold reduction in the Src caveolar localization (Fig. 4D). Again this effect was dependent on clathrin association with Tom1L1 as CHC down-regulation restored Src caveolar distribution. Similarly, mutation of the CHC binding sites in Tom1L1 (ΔL/L401A) abrogated this effect. Collectively, these data support the idea that the CHC-Tom1L1 complex acts as a negative regulator of SFK caveolar localization.

Tom1L1-CHC inhibits SFK-PDGF receptor association in caveolae and mitogenesis.

The biological meaning of SFK membrane partitioning was next investigated in PDGF-stimulated NIH 3T3 cells, as we have previously reported that SFK directly associate with activated PDGFR in caveolae to regulate mitogenic signaling (27, 28). Tom1L1 overexpression reduced SFK levels in CEF of PDGF-stimulated NIH 3T3 cells (Fig. 5A, left panels). No changes were detected on the whole level of SFK, excluding a protein degradation mechanism (Fig. 5C). In contrast, PDGFR activity was not affected in these

fractions (Fig. 5B), confirming that Tom1L1 does not regulate partitioning of this receptor at the plasma membrane. Tom1L1-induced SFK caveolar depletion was reversed by CHC down-regulation or by mutation of CHC binding sites in Tom1L1 (ΔL/L401A) (Fig.5B). These observations are consistent with a Tom1L1-CHC inhibitory mechanism in PDGF-stimulated fibroblasts. Therefore, we hypothesized that, due to SFK delocalization, Tom1L1 should reduce SFK-PDGFR complex formation in caveolae. Association of PDGFR with SFK was revealed by in vitro kinase assay of immunoprecipitated SFK from CEF (Fig. 5A, left panel). As previously reported (27), phosphorylated SFK was detected in association with a 180 KDa phospho-protein, which was further identified as the PDGFR by re-imunoprecipitation with a specific antibody (Fig. 5A, right panel). Moreover, Tom1L1 overexpression reduced the level of SFK-PDGFR complexes in CEF. As expected, this effect was abolished by down-regulation of CHC or mutation of the CHC binding sites in Tom1L1. We concluded that the effect of Tom1L1 on SFK-PDGFR complex formation is primarily due to a reduction of SFK in caveolae. Higher over-expression of this adapter may additionally compete with the receptor for association with SFK (8).

The role of CHC on Tom1L1 biological activity was next assessed on mitogenic response induced by a low concentration of PDGF (Fig. 5D and E). DNA synthesis was monitored by adding bromo-deoxyuridine (BrdU) in the medium. We found that PDGF induced a 30% BrdU incorporation and that retroviral expression of Tom1L1 abolished this cellular response (Fig. 5D). Like previously reported with Tom1L1 (8), CHC down-regulation enhanced S phase entry both in quiescent and stimulated cells. This was consistent with a better SFK-PDGFR coupling observed in caveolae (Fig. 5A) and an increase in Src mitogenic signaling (MF and SR, unpublished data). Most importantly, Tom1L1 mitogenic inhibition was not observed any longer in cells with reduced level of CHC. Nonetheless, these cells still required SFK activities for mitogenic signaling as the SFK inhibitor SU6656, still inhibited

PDGF-induced DNA synthesis (Fig. 5D). This suggested that Tom1L1 inhibits mitogenesis by a CHC-dependent mechanism. This hypothesis was further confirmed by the absence of inhibitory effect observed with the ΔL/L401A mutant, which still associates with Src but not CHC (Fig. 5E). Therefore, the negative effect on the mitogenic response of Tom1L1 is dependent upon its association with CHC.

Tom1L1-CHC affects oncogenic Src membrane partitioning, Src mitogenic and transforming activities.

We then asked whether a similar regulation occurs in the presence oncogenic Src. We first looked at the level of avian SrcY527F in CEF from HEK 293 cells expressing low level of this kinase. As shown in Fig. 6A, SrcY527F was readily detected in caveolar fractions. Again, Tom1L1 over-expression strongly reduced Src level without affecting caveolin accumulation. Inhibition was due to SrcY527F de-localization as Tom1L1 did not have an effect on the whole level of the protein. Quantification of these experiments indicated that up to 70% of the expressed Src was excluded from caveolae fractions. Interestingly, this exclusion was largely reduced when the Tom1L1 mutant ΔL/L401A was used, indicating that this activity is dependent on its association with CHC. The impact of membrane compartimentation was next investigated on SrcY527F mitogenic signaling in the absence of extracellular stimuli. NIH 3T3 cells stably expressing a low level of SrcY527F (Src 527-NIH 3T3) were serum-starved for 30 h and then BrdU was added for an extra 18 h in order to record de novo DNA synthesis. In these conditions, 75% of the cells incorporated BrdU (Fig. 5B). We then addressed the role of cholesterol-enriched microdomains on this cellular response. The amino-terminal truncated mutant of caveolin-3, Cav-3DGV, has been described to reduce both caveolae and cholesterol level from the plasma membrane (24, 27). We have also observed that this mutant blocks Src mitogenic signaling induced by PDGF (27).

Interestingly, Cav-3DGV inhibited SrcY527F-driven DNA synthesis (Fig. 6B), suggesting that membrane cholesterol-enriched domains regulate this Src biological activity. The role of the Tom1L1-CHC complex was next investigated on this cellular response. Tom1L1 reduced SrcY527F-induced BrdU incorporation by 70%. Inhibition was dependent on the association with CHC as no significant effect was observed with ΔL/L401A. In the presence of higher levels of SrcY527F, this inhibitory effect can be completely abolished (8). This may be explained by the inability of the Tom1L1-CHC complex to deplete enough Src from the cholesterol-enriched microdomains to prevent mitogenic signaling (GC and SR, unpublished data). The influence of the Tom1L1-CHC complex was also tested on Src transforming activity. SrcY527F was transduced by retroviral infection in NIH 3T3 cells for efficient foci induction. CMV-driven SrcY527F expression exhibited lower biological activity in this assay, probably due to active protein degradation (GC and SR, unpublished data). Co-infection of Tom1L1 viruses reduced foci induction by 60 % (Fig. 6C). This inhibition was largely overcome by CHC down-regulation (siRNA CHC) or by using the Tom1L1 mutant which cannot associate with CHC (ΔL/L401A), suggesting that Tom1L1 inhibitory effect is dependent upon its association with CHC. Therefore Tom1L1-CHC also inhibits Src transforming activity, in addition to Src-driven DNA synthesis.

Tom1L1 that does not associate with CHC accumulates in caveolae and promotes Src-driven DNA synthesis.

We next investigated the impact of CHC on Tom1L1 membrane distribution. Tom1L1 was barely detected in CEF when expressed in HEK 293 cells (Fig. 7A and B). However, down-regulation of CHC increased the level of Tom1L1 in CEF by 3.5 while not affecting that of caveolin. Accordingly, a 4 fold higher level of ΔL/L401A was observed in caveolae fractions when compared to the wild-type protein. These results were next confirmed with an

immunofluorescence approach in fibroblasts: while less than 25% of cells showed co-localization of Tom1L1 with caveolin at the cell periphery, CHC knock-down increased this percentage by 2 fold and a similar scenario was observed when CHC binding sites in Tom1L1 were deleted (Fig. 7B, right panel). We thus concluded that Tom1L1 is mostly excluded from caveolae when in association with CHC.

The biological significance of Tom1L1 accumulation in caveolae was next investigated on Src-driven DNA synthesis (Fig. 8A). As previously reported, wild-type Src did not induce BrdU incorporation even in the presence of Tom1L1 (8). In contrast, the Tom1L1 mutant ΔL/L401A, which does not associate with CHC, increased BrdU incorporation by 20%. This suggested that the inability of Tom1L1 to promote Src mitogenic signaling was due to its association with clathrin. The moderate effect obtained with ΔL/L401A could be due to the absence of the linker sequence that has been also implicated in the interaction and activation of Src (8). The negative role of the association with CHC on DNA synthesis was confirmed by a siRNA approach. While Src *per se* still had no effect in CHC-depleted cells, Tom1L1 promoted Src-driven DNA synthesis for 20% of expressing cells. We next addressed the specificity of CHC inhibition. The middle T antigen of the polyoma virus (mT) is another interactor and activator of Src catalytic activity. In vivo, mT promotes Src mitogenic and transforming activity (11). Accordingly, mT triggered Src-driven DNA synthesis in 40% of expressing cells; however this effect was not increased by CHC depletion (Fig. 8B). We hypothesized that the capacity of mT to induce Src mitogenic activity was due to its localization in cholesterol-enriched microdomains. Indeed, mT was preferentially found in caveolar enriched fractions (Fig. 8C), unlikely from Tom1L1, whose membrane partitioning is regulated by CHC. We concluded that the inability of Tom1L1 to induce Src mitogenic signaling was related to its exclusion from caveolae due to its association with CHC. Finally, we wished to confirm the role of endogenous Src on this

cellular process. We noticed that CHC depletion alone enhanced DNA synthesis from 10 to 15 % (Fig. 8D). This cellular effect was abrogated by treatment of the SFK inhibitor SU6656 and expression of the Cav-3DGV mutant, implicating a Src mitogenic signaling regulated by caveolae and/or membrane cholesterol. Similarly, we found that Tom1L1 alone also enhanced DNA synthesis in cells with reduced CHC that was inhibited by the SFK inhibitor SU6656 (Fig. 8D). We concluded that Tom1L1 interacts with endogenous Src when present in caveolae for DNA synthesis induction.

DISCUSSION

SFK play important roles in signal transduction induced by growth factors and they are subjected to complex regulation for specific signaling including catalytic activation, substrate specificity and sub-cellular compartmentalization (5, 28). Our results point to membrane cholesterol-enriched domains as important regulators of Src proliferative function both upon a physiological (PDGF) and oncogenic activation (SrcY527F, mT of polyoma virus). We have identified a novel mechanism of negative regulation of Src proliferative and transforming activities through depletion of SFK from cholesterol-enriched domains. By associating with the complex Tom1L1-CHC, Src is de-localized from these organelles, thus preventing association with growth factor receptors to induced mitogenic signals. Alternatively exclusion of oncogenic Src from cholesterol-enriched membrane below a threshold may prevent the induction of DNA synthesis and foci formation. This mechanism may have important implications for Src signaling specificity (i.e. proliferation versus differentiation) and during tumorigenesis (8, 15). This may also explain why Tom1L1 does not promote Src mitogenic and/or oncogenic function while strongly stimulating catalytic activity in vitro. One can hypothesize that other Src activators, which do not localize in

cholesterol-enriched microdomains, could also not promote Src mitogenic and transforming activities.

Finally, this report raises important issues regarding the mechanism and the function of SFK de-localization by Tom1L1-CHC. Our data suggest that CHC is primarily responsible for Src exclusion from caveolae. Tom1L1-Tyr457 phosphorylation by Src may increase ternary complex formation for efficient delocalization of the kinase. Finally, the nature of Src vesicular re-localization has not been investigated in this study. Nevertheless, the association with CHC strongly suggests that it could accumulate in clathrin-coated vesicle for endocytosis of membrane receptors to be identified. While probably not involved in PDGF receptor internalization (GC and CB, unpublished data), CHC and Tom1L1 have been implicated in EGFR endocytosis (14, 21) and our data suggests that Tom1L1 allows CHC phosphorylation by Src for enhanced receptor internalization (29). Therefore, the balance between SFK localization in cholesterol-enriched microdomains and clathrin-coated vesicles may play a crucial role for normal and tumor cell growth.

ACKNOWLEDGEMENTS

We thank P. Coopman, D. Drubin, A. Kazlauskas and J. Keen for various reagents, P. Jouin and J. Poncet for mass spectrometric analysis, the RIO platform for imaging analysis, W.J. Hong for sharing unpublished data and our colleagues for critical reading of the manuscript. This work was supported by grants of the CNRS, University of Montpellier II, INCa and ARC. MF was supported by the ARC. GC is supported by the "Ligue Nationale Contre le Cancer". CB and SR are INSERM investigators.

REFERENCES

1. **Blake, R. A., M. A. Broome, X. Liu, J. Wu, M. Gishizky, L. Sun, and S. A. Courtneidge.** 2000. SU6656, a selective src family kinase inhibitor, used To probe growth factor signaling. Mol Cell Biol **20:**9018-27.

2. **Boggon, T. J., and M. J. Eck.** 2004. Structure and regulation of Src family kinases. Oncogene **23:**7918-27.

3. **Bonifacino, J. S.** 2004. The GGA proteins: adaptors on the move. Nat Rev Mol Cell Biol **5:**23-32.

4. **Boureux, A., O. Furstoss, V. Simon, and S. Roche.** 2005. c-Abl tyrosine kinase regulates a Rac/JNK and a Rac/Nox pathway for DNA synthesis and c-myc expression induced by growth factors. J. Cell Science **118:**3717-3726.

5. **Bromann, P. A., H. Korkaya, and S. A. Courtneidge.** 2004. The interplay between Src family kinases and receptor tyrosine kinases. Oncogene **23:**7957-68.

6. **Douglass, A. D., and R. D. Vale.** 2005. Single-molecule microscopy reveals plasma membrane microdomains created by protein-protein networks that exclude or trap signaling molecules in T cells. Cell **121:**937-50.

7. **Engqvist-Goldstein, A. E., R. A. Warren, M. M. Kessels, J. H. Keen, J. Heuser, and D. G. Drubin.** 2001. The actin-binding protein Hip1R associates with clathrin during early stages of endocytosis and promotes clathrin assembly in vitro. J Cell Biol **154:**1209-23.

8. **Franco, M., O. Furstoss, V. Simon, C. Benistant, W. J. Hong, and S. Roche.** 2006. The adaptor protien Tom1L1 is a negative regulator of Src mitogenic signaling induced by growth factors. Mol Biol Cell **26:**1932-1947.

9. **Furstoss, O., K. Dorey, V. Simon, D. Barilla, G. Superti-Furga, and S. Roche.** 2002. c-Abl is an effector of Src for growth factor-induced c-myc expression and DNA synthesis. EMBO J **27:**514-524.

10. **Huang, F., A. Khvorova, W. Marshall, and A. Sorkin.** 2004. Analysis of clathrin-mediated endocytosis of epidermal growth factor receptor by RNA interference. J Biol Chem **279:**16657-61.

11. **Ichaso, N., and S. M. Dilworth.** 2001. Cell transformation by the middle T-antigen of polyoma virus. Oncogene **20:**7908-16.

12. **Katoh, Y., H. Imakagura, M. Futatsumori, and K. Nakayama.** 2006. Recruitment of clathrin onto endosomes by the Tom1-Tollip complex. Biochem Biophys Res Commun **341:**143-9.

13. **Lassaux, A., M. Sitbon, and J. L. Battini.** 2005. Residues in the murine leukemia virus capsid that differentially govern resistance to mouse Fv1 and human Ref1 restrictions. J Virol **79:**6560-4.

14. **Le Roy, C., and J. L. Wrana.** 2005. Clathrin- and non-clathrin-mediated endocytic regulation of cell signalling. Nat Rev Mol Cell Biol **6:**112-26.

15. **Li, W., C. Marshall, L. Mei, L. Dzubow, C. Schmults, M. Dans, and J. Seykora.** 2005. Srcasm modulates EGF and Src-kinase signaling in keratinocytes. J Biol Chem **280:**6036-46.

16. **Lohi, O., A. Poussu, Y. Mao, F. Quiocho, and V. P. Lehto.** 2002. VHS domain -- a longshoreman of vesicle lines. FEBS Lett **513:**19-23.

17. **Martin, G. S.** 2001. The hunting of the Src. Nat Rev Mol Cell Biol **2:**467-75.

18. **Munro, S.** 2003. Lipid rafts: elusive or illusive? Cell **115:**377-88.

19. **Pike, L. J.** 2005. Growth factor receptors, lipid rafts and caveolae: An evolving story. Biochim Biophys Acta **9:**9.

20. **Pol, A., S. Martin, M. A. Fernandez, M. Ingelmo-Torres, C. Ferguson, C. Enrich, and R. G. Parton.** 2005. Cholesterol and fatty acids regulate dynamic caveolin trafficking through the Golgi complex and between the cell surface and lipid bodies. Mol Biol Cell **16:**2091-105.

21. **Puertollano, R.** 2005. Interactions of TOM1L1 with the multivesicular body sorting machinery. J Biol Chem **280:**9258-64.

22. **Puri, C., D. Tosoni, R. Comai, A. Rabellino, D. Segat, F. Caneva, P. Luzzi, P. P. Di Fiore, and C. Tacchetti.** 2005. Relationships between EGFR signaling-competent and endocytosis-competent membrane microdomains. Mol Biol Cell **16:**2704-18.

23. **Roche, S., G. Alonso, A. Kazlauskas, V. M. Dixit, S. A. Courtneidge, and A. Pandey.** 1998. Src-like adaptor protein (Slap) is a negative regulator of mitogenesis. Curr Biol **8:**975-8.

24. **Roy, S., R. Luetterforst, A. Harding, A. Apolloni, M. Etheridge, E. Stang, B. Rolls, J. F. Hancock, and R. G. Parton.** 1999. Dominant-negative caveolin inhibits H-Ras function by disrupting cholesterol-rich plasma membrane domains. Nat Cell Biol **1:**98-105.

25. **Seykora, J. T., L. Mei, G. P. Dotto, and P. L. Stein.** 2002. 'Srcasm: a novel Src activating and signaling molecule. J Biol Chem **277:**2812-22.

26. **Simons, K., and D. Toomre.** 2000. Lipid rafts and signal transduction. Nat Rev Mol Cell Biol **1:**31-9.

27. **Veracini, L., M. Franco, A. Boureux, V. Simon, S. Roche, and C. Benistant.** 2006. Two distinct pools of Src family tyrosine kinases regulate PDGF-induced DNA synthesis and actin dorsal ruffles. J Cell Sci **20:**2921-34.

28. **Veracini, L., M. Franco, A. Boureux, V. Simon, S. Roche, and C. Benistant.** 2005. Two functionally distinct pools of Src kinases for PDGF receptor signalling. Biochem Soc Trans **33:**1313-5.

29. **Wilde, A., E. C. Beattie, L. Lem, D. A. Riethof, S. H. Liu, W. C. Mobley, P. Soriano, and F. M. Brodsky.** 1999. EGF receptor signaling stimulates SRC kinase phosphorylation of clathrin, influencing clathrin redistribution and EGF uptake. Cell **96:**677-87.

30. **Zyss, D., P. Montcourrier, B. Vidal, C. Anguille, F. Merezegue, A. Sahuquet, P. H. Mangeat, and P. J. Coopman.** 2005. The Syk tyrosine kinase localizes to the centrosomes and negatively affects mitotic progression. Cancer Res **65:**10872-80.

FIGURE LEGENDS

Figure 1. Association of CHC with Tom1L1.

A. Modular structure of Tom1L1 wild-type and of the mutants used in this study. The VHS and GAT homology domains, the linker region and the C-terminus (C) are indicated. Src binding sites (i.e. $PP_{421}LP$ and Tyr457), the mutations of these Src binding sites (i.e. $A_{420}ALA$ and Phe457 in Tom1L1YPP) and the mutation of the CHC binding site $A_{401}AQPSVA$ (in ΔL/L401A) are indicated. **B.** Association of CHC with Tom1L1 in vitro. HeLa-cell lysates were incubated with the indicated Gst fusions proteins or control Gst beads and the presence of CHC in the pull-down assays were revealed by Western blotting with a specific antibody. Input (15% of the cell-lysate) was loaded as a positive control. **C**. Association of CHC with Tom1L1 in NIH 3T3 cells. CHC level associated with Tom1L1 in NIH 3T3 cells was assessed by Western blotting with anti-CHC antibody after immunoprecipitation of Tom1L1 with control (IgG) or anti-Tom1.3 antibody as shown. The level of immunoprecipitated Tom1L1 is also shown.

Figure 2. CHC-Tom1L1 complex formation

A. Association of CHC with Tom1L1 involves both the Linker and the C-terminus sequences. HEK 293 cells were transfected with CHC-DsRed and the indicated Tom1L1 constructs. Tom1L1 proteins were immunoprecipitated with the anti-Tom1L1.3 antibodies and the presence of associated CHC-DsRed was revealed by Western-blotting with anti-CHC antibodies. The levels of associated CHC-Ds-Red, immunoprecipitated Tom1L1 and expressed CHC-DsRed are shown. **B.** In vitro association of Tom1L1 with CHC terminal domain Gst fusion protein (Gst-CHC-TD). Indicated fusion protein bound to glutathione beads was incubated with the purified Tom1L1. The presence of Tom1L1 was revealed by Western blotting with the indicated antibody. **C**. Association of Tom1L1 C-terminus with

CHC involves a Leu-rich motif at the C-terminus. HeLa-cell lysates were incubated with indicated Gst fusions proteins or control Gst beads and the interaction with CHC was revealed by Western blotting with a specific antibody**.** Input (5% of the cell lysates) was included as a positive control. **D**. Regulation of CHC-Tom1L1 complex formation by the Linker and the Leu-rich motif L_{401}LQPSVL. Tom1L1 was immunoprecipitated from lysates of HEK 293 cells transiently expressing the indicated constructs with the anti-Tom1L1.3 antibodies or a control IgG and the presence of associated CHC was revealed by Western-blotting using anti-CHC antibodies. The level of expressed and associated CHC, and immunoprecipitated Tom1L1 are shown. **E**. Co-localization of CHC with Tom1L1. Representative fluorescence of CHC-DsRed, GFP-Tom1L1 (top panels) or GFP-Tom1L1 mutant that does not associate with CHC (ΔL/L401A) (bottom panel), and the merge is shown of a co-tranfected NIH 3T3 cell as obtained after deconvolution (Huygens software).

Figure 3. CHC-Tom1L1-Src ternary complex formation.

A. Src-CHC-Tom1L1 ternary complex formation in vitro. Association of indicated purified proteins with Gst-CHC-TD bound to beads. The presence of Src, phosphorylated Src and phosphorylated Tom1L1 were shown by Western blotting with the indicated antibodies. Association of Gst-CHC-TD with Tom1L1 was revealed by Brilliant Blue staining of the complex separated on a SDS-PAGE gel. **B**. Src-CHC-Tom1L1 complex formation in HEK 293 cells that co-express Src and Tom1L1. Each member of the complex was immunoprecipitated with the indicated antibodies and the presence of co-associated protein was detected by western blotting with shown antibodies. Tyrosine phosphorylation content of each immunoprecipitate is shown. Level of tyrosine phosphorylated proteins, CHC, SFK and Tom1L1 are also shown from a whole cell lysate (WCL). **C.** Endogenous Tom1L1 bridges SFK to CHC in NIH 3T3 cells. CHC level associated with SFK was assessed by Western

blotting with the indicated antibody after immunoprecipitation of SFK from NIH 3T3 cells that were transfected with the indicated siRNA. The levels of SFK, Tom1L1 and tubulin are also shown. Quantification of associated CHC is indicated. **D**. Co-localization of Src, Tom1L1 and CHC. Representative fluorescences of CHC-DsRed, GFP-Tom1L1 and immunostained avian Src are shown with the merge of a NIH 3T3 cell co-expressing all 3 components after deconvolution, as described in Materials and Methods section. **E.** SFK phosphorylate CHC-TD in the presence of Tom1L1. In vitro kinase assay using purified Src or Fyn as shown and in the presence of the indicated concentrations of CHC-TD and 1 μM of Gst or Gst-Tom1L1 as indicated. Labeled SFK, Gst-Tom1L1 and CHC-TD are shown. **F.** Tom1L1 regulates Src-induced CHC phosphorylation in Src-transformed cells. CHC was immunoprecipitated from NIH 3T3 cells or NIH3 3T3 cells stably expressing SrcY527F (Src 527) as shown and that were transfected with control or siRNA Tom1L1 as indicated. The level of CHC and tyrosine phosphorylated CHC (pY-CHC) is shown and was assessed by Western blotting with indicated antibodies. The level of Tom1L1 and tubulin from indicated cell-lysates (WCL) is also shown.

Figure 4. Tom1L1 reduces SFK localization in caveolae through CHC association.

A. Tom1L1 reduces SFK but not PDGFR level in CEF. Levels of SFK, PDGFR and caveolin in CEF purified from HEK 293 cells that were transfected with the indicated constructs, and control or CHC siRNAs when indicated. The levels of expressed SFK, PDGFR and Tom1L1 from the whole-cell lysate (WCL) are also shown. **B**. Quantitative analysis of SFK and PDGFR level in CEF obtained from two independent experiments. **C.** Depletion of Tom1L1 enhances SFK accumulation in CEF. SFK and caveolin levels in CEF and soluble fractions (fractions 7-9, "soluble") purified from HEK 293 cells that were infected mock (shRNA Luciferase) or shRNA Tom1L1 as indicated. The level of tubulin and Tom1L1 is also shown.

A representative example (**D**) and its statistical analysis (**E**) (mean ± SD, n = 3) of Src/caveolin co-localization at the periphery of NIH 3T3 cells. Cells infected with control (mock) or indicated Tom1L1 retroviruses were seeded on coverslips and transfected with avian Src together with siRNA (when indicated) for 48 hours. Cells were then fixed and processed for immunofluorescence as described in the Materials and Methods section. Is shown a representative example of avian Src immunostaining, caveolin immunostaining and the merge from indicated infected NIH 3T3 cells and obtained by confocal analysis as described in the Material and Methods section. A three fold magnification of the merge at the cell periphery is also included. The percentage of transfected cells that exhibited Src/caveolin co-localization at the cell periphery was calculated as described in Material and Methods section. Results are expressed as the mean ± SD of 3 independent experiments. The levels of Tom1L1 and CHC are shown in Fig 4A.

Figure 5. Tom1L1-CHC inhibits SFK-PDGFR coupling in caveolae and PDGF-induced DNA synthesis. **A.** The Tom1L1-CHC complex inhibits SFK-PDGFR complex formation in caveolae. In vitro kinase assays of immunoprecipitated SFK (left panel) are shown from CEF purified from PDGF stimulated NIH 3T3 cells that were infected with control (mock) or indicated viruses and transfected with control or CHC siRNA when indicated. Level of caveolin and quantified level of SFK in CEF are shown. Right panel: re-immunoprecipitation of the labeled 180KDa protein observed in SFK immunoprecipitate with the PDGFR beta specific PR4 antibody. Labeled PDGFR and SFK are shown. **B.** The Tom1L1-CHC does not affect PDGFR activity in caveolae. In vitro kinase assays of immunoprecipitated PDGFR beta with indicated antibody is shown from CEF purified from PDGF-stimulated NIH 3T3 cells that were infected with control (mock) or indicated viruses and transfected with control or CHC siRNA when indicated. The level of caveolin in CEF is shown **C.** Levels of CHC,

Tom1L1, SFK and tubulin are shown from whole cell-lysates of NIH 3T3 cells infected with control (mock) or indicated viruses and transfected with control or CHC siRNAs when indicated**. D**. PDGF mitogenic inhibition induced by Tom1L1 requires association with CHC. NIH 3T3 cells seeded onto coverslips and transfected or not with indicated constructs or siRNA were made quiescent by serum starvation for 30 h, treated or not with the SFK inhibitor SU6656 (2 μM) and stimulated or not with PDGF (5 ng/ml) as indicated, in the presence of BrdU for 18 h. Cells were then fixed and processed for immunofluorescence. The percentage of transfected cells that incorporated BrdU was calculated as described in the Material and Methods section. Results are expressed as the mean ± SD of 3-5 independent experiments.

Figure 6. Tom1L1-CHC affects SrcY527F membrane partitioning, SrcY527F-induced DNA synthesis and foci formation.

A. Tom1L1-CHC reduces SrcY527F level in CEF. Levels of avian Src and caveolin from CEF purified from HEK 293 that were transfected with SrcY527F together or not with the indicated Tom1L1 constructs. The levels of expressed Src, Tom1L1 and tubulin are shown from the whole-cell lysate (WCL). **B**. Tom1L1-CHC inhibits Src-driven DNA synthesis. NIH 3T3 cells stably transformed by SrcY527F (Src 527) seeded onto coverslips and transfected or not with indicated constructs were incubated in 0.5 % serum for 30 h and further incubated in the presence of BrdU for 18 h. Cells were then fixed and processed for immunofluorescence. The percentage of transfected cells that incorporated BrdU was calculated as described in the Material and Methods section. Results are expressed as the mean ± SD of 3 independent experiments. **C** Tom1L1-CHC inhibits SrcY527F transforming activity. The statistical analysis of inhibition of SrcY527F-induced foci by Tom1L1-CHC is shown. NIH 3T3 cells were transfected or not with siRNA CHC as shown, then infected with control (mock) or

indicated retroviruses. After 12 days of growth, foci were stained and scored as described in the Materials and Methods section. Foci formation (% of foci obtained relative to foci induced by SrcY527F) is represented as the mean ± SD of 3 independent experiments

Figure 7. Tom1L1 that does not associate with CHC accumulates in caveolae.

A and **B**. Tom1L1 that does not associate with CHC accumulates in caveolae. (A) Tom1L1 and caveolin levels in CEF of HEK 293 cells transfected with Tom1L1 constructs and control or CHC siRNAs, when indicated. The levels of CHC, Tom1L1 and tubulin from the whole-cell lysate (WCL) are also shown. (B) Left panel: statistical analysis (mean ± SD, n = 3) of the percentage of Tom1L1 level in CEF shown in panel A. Right panel: statistical analysis of Tom1L1/caveolin co-localization at the periphery of NIH 3T3. Cells seeded on coverslips were transfected with indicated Tom1L1 construct together or not with indicated siRNA for 48 hours. Cells were then fixed and processed for immunofluorescence as described in the Materials and Methods section. The percentage of transfected cells that exhibited Tom1L1/caveolin co-localization at the cell periphery was calculated as described in Material and Methods section. Results are expressed as the mean ± SD of 3 independent experiments

Figure 8. Tom1L1 that does not associate with CHC increases Src-driven DNA synthesis.

A. Tom1L1 that does not associate with CHC increases wild-type Src-driven DNA synthesis. NIH 3T3 cells seeded onto coverslips and transfected or not with the indicated Tom1L1 constructs and CHC siRNA, as indicated, were incubated in 0.5 % serum for 30 h and further incubated in the presence of BrdU for 18 h. Cells were then fixed and processed for immunofluorescence. **B.** CHC does not regulate the capacity of mT to enhance Src-driven DNA synthesis. BrdU incorporation (mean ± SD, n = 4) of serum-starved NIH 3T3 cells that

were transfected with indicated constructs and the indicated siRNAs when shown. **C.** mT is preferentially localized in CEF. Level of mT in CEF and soluble fractions (fractions 7-9, "soluble") from HEK 293 cells expressing mT. The level of caveolin is also shown. **D.** Tom1L1 enhances DNA synthesis in CHC-depleted NIH 3T3 cells in a Src-dependant manner. NIH 3T3 cells seeded onto coverslips and transfected or not with the indicated constructs and CHC siRNA, as indicated, were incubated in 0.5 % serum for 30 h, treated or not with SU6656 (2 μM) as shown and further incubated in the presence of BrdU for 18 h. Cells were then fixed and processed for immunofluorescence. The percentage of transfected cells that incorporated BrdU was calculated as described in the Material and Methods section. The percentage of transfected cells that incorporated BrdU was calculated as described in the Material and Methods section. Results are expressed as the mean ± SD of 3-4 independent experiments. *$P < 0.05$ and **$P < 0.01$ using a student's *t*-test.

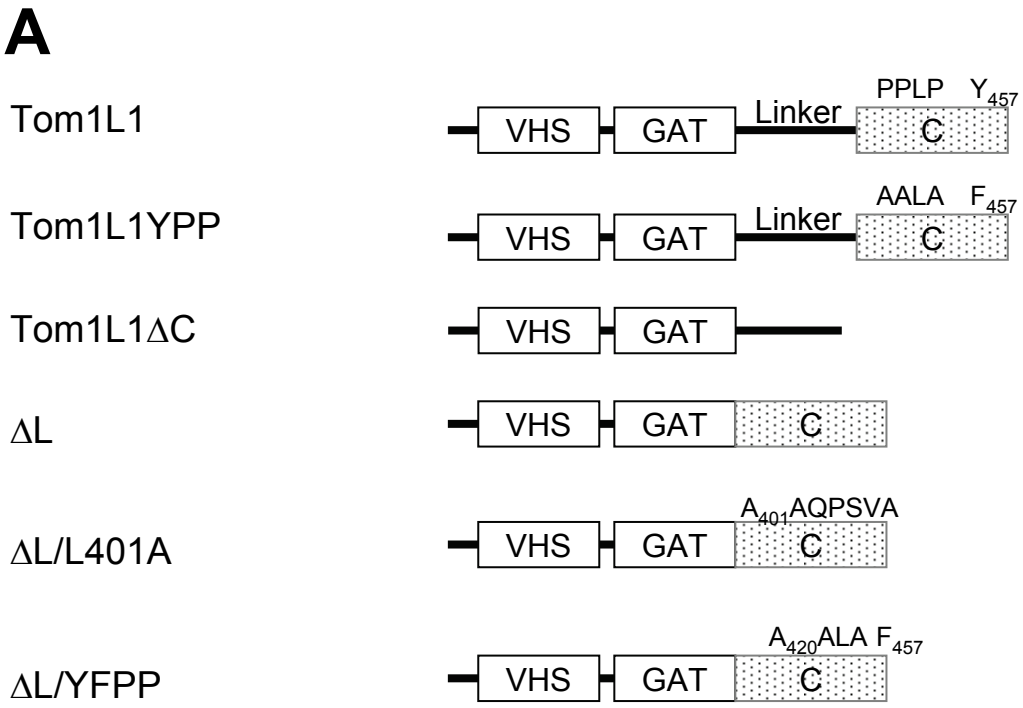
A
Tom1L1
VHS
GAT
Linker
PPLP Y457
C
Tom1L1YPP
AALA F457
ΔL
ΔL/L401A
A401AQPSVA
ΔL/YFPP
A420ALA F457

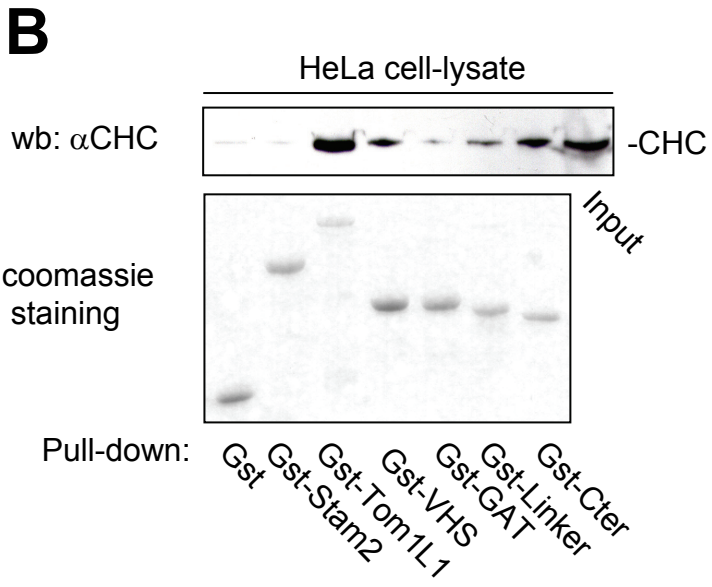
B
HeLa cell-lysate
wb: αCHC
-CHC
Input
coomassie staining
Pull-down:
Gst
Gst-Stam2
Gst-Tom1L1
Gst-VHS
Gst-GAT
Gst-Linker
Gst-Cter

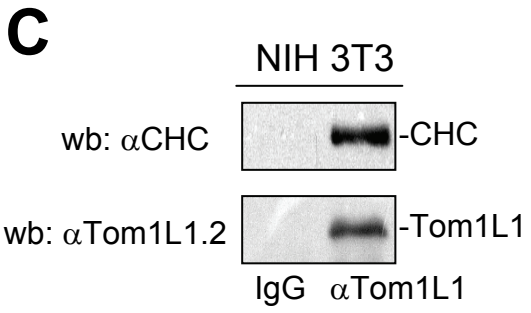
C
NIH 3T3
wb: αCHC
-CHC
wb: αTom1L1.2
-Tom1L1
IgG
αTom1L1

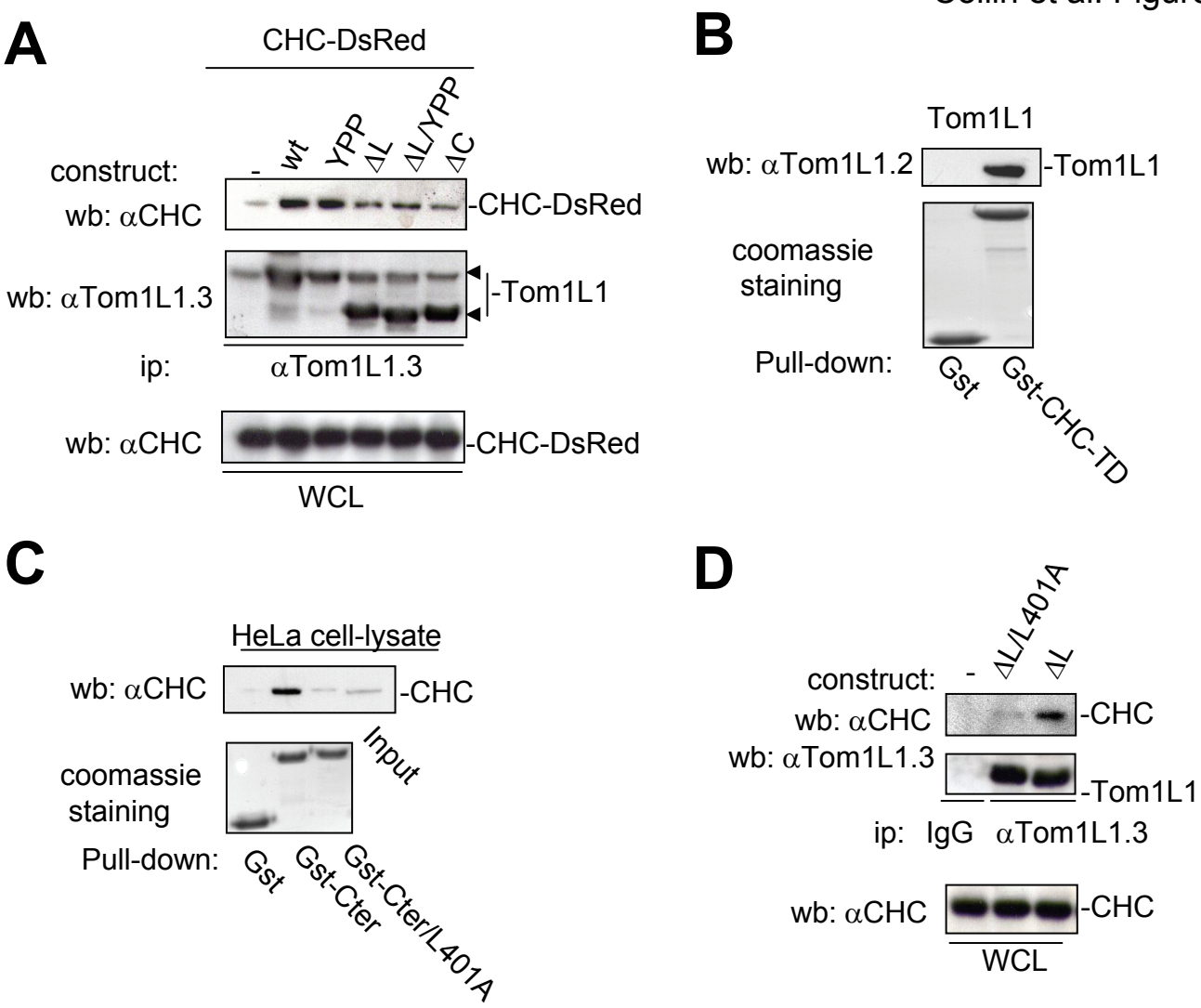
A
CHC-DsRed
construct:
-
wt
YPP
ΔL
ΔL/YPP
ΔC
wb: αCHC
-CHC-DsRed
wb: αTom1L1.3
-Tom1L1
ip:
αTom1L1.3
wb: αCHC
-CHC-DsRed
WCL
B
Tom1L1
wb: αTom1L1.2
-Tom1L1
coomassie staining
Pull-down:
Gst
Gst-CHC-TD
C
HeLa cell-lysate
wb: αCHC
-CHC
Input
coomassie staining
Pull-down:
Gst
Gst-Cter
Gst-Cter/L401A
D
construct:
-
ΔL/L401A
ΔL
wb: αCHC
-CHC
wb: αTom1L1.3
-Tom1L1
ip:
IgG
αTom1L1.3
wb: αCHC
-CHC
WCL

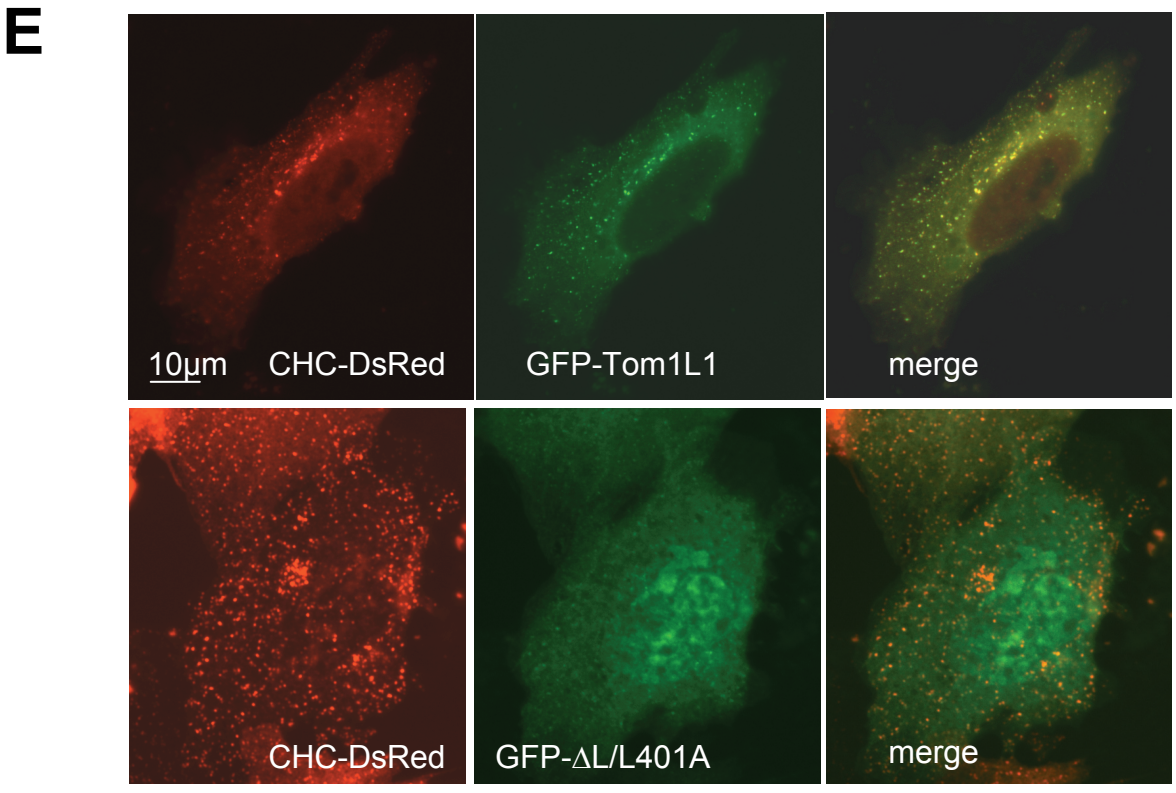
E
10µm
CHC-DsRed
GFP-Tom1L1
merge
CHC-DsRed
GFP-ΔL/L401A
merge

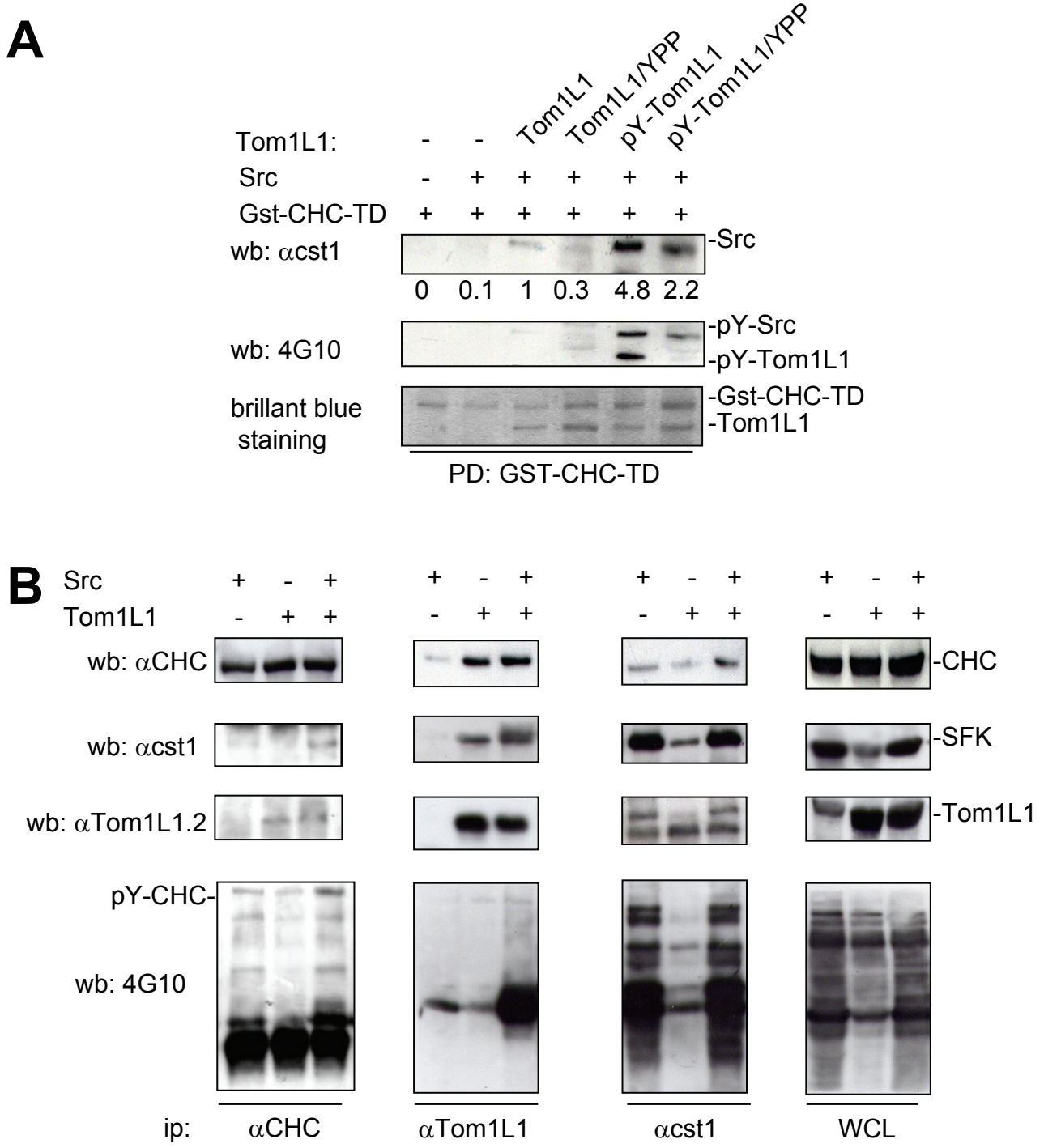
A
Tom1L1:
Src
Gst-CHC-TD
Tom1L1
Tom1L1/YPP
pY-Tom1L1
pY-Tom1L1/YPP
wb: αcst1
-Src
0 0.1 1 0.3 4.8 2.2
wb: 4G10
-pY-Src
-pY-Tom1L1
brillant blue staining
-Gst-CHC-TD
-Tom1L1
PD: GST-CHC-TD
B
Src
Tom1L1
wb: αCHC
-CHC
wb: αcst1
-SFK
wb: αTom1L1.2
-Tom1L1
pY-CHC-
wb: 4G10
ip: αCHC
αTom1L1
αcst1
WCL
C
NIH 3T3
siRNA:
control
Tom1L1
wb: αCHC
-CHC
1.0 0.3
wb: αcst1
-SFK
αcst1
NIH 3T3
control
Tom1L1
wb: αTom1L1.2
-Tom1L1
αTom1L1
wb: αtubulin
-tubulin
WCL

D

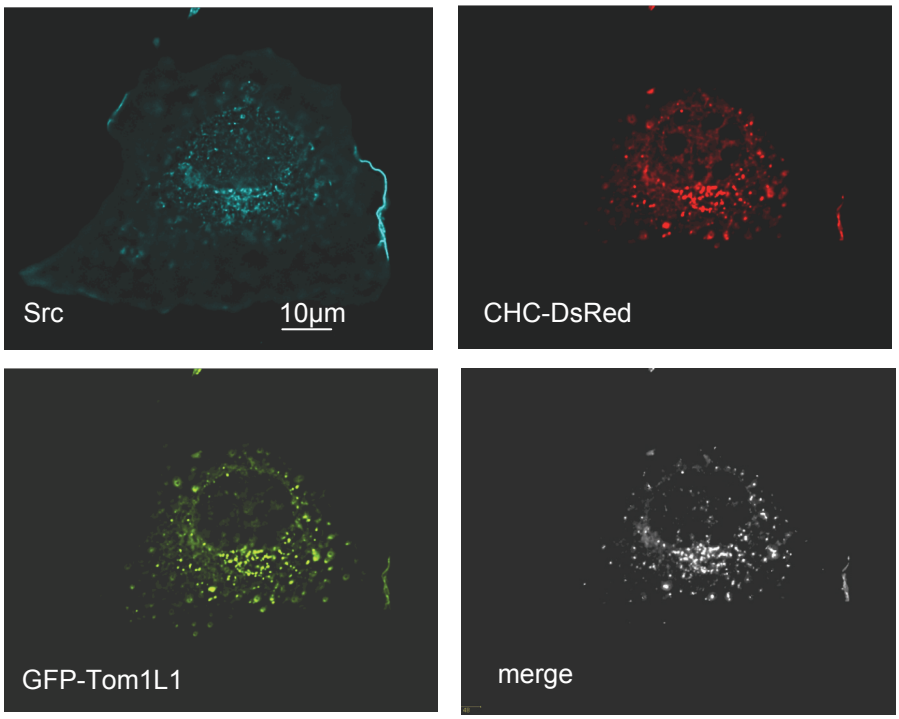
Src
10µm
CHC-DsRed
GFP-Tom1L1
merge

E

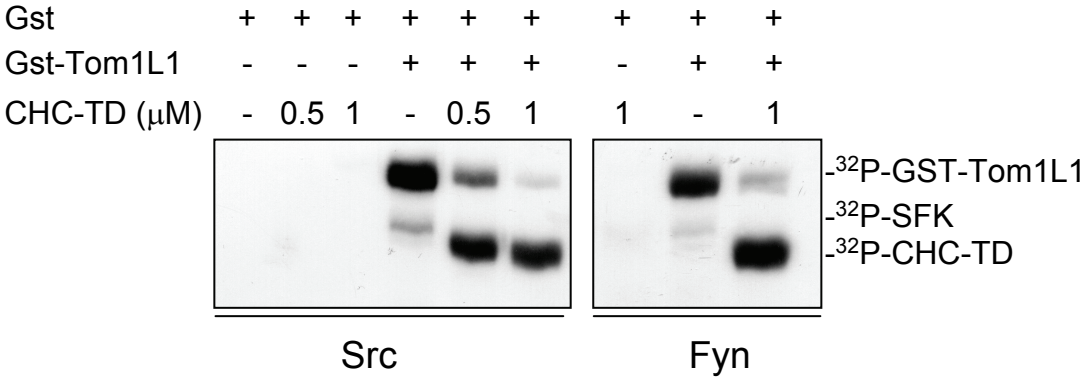
Gst + + + + + + + + +
Gst-Tom1L1 - - - + + + - + +
CHC-TD (µM) - 0.5 1 - 0.5 1 1 - 1
-32P-GST-Tom1L1
-32P-SFK
-32P-CHC-TD
Src
Fyn

F

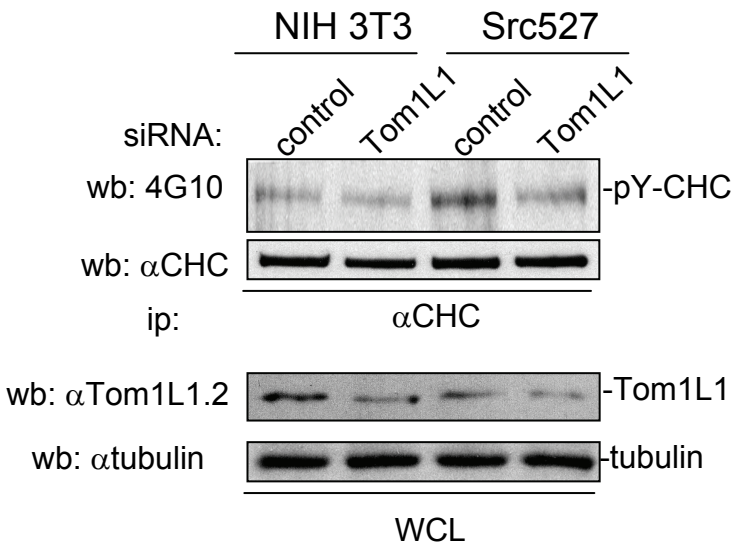
NIH 3T3
Src527
siRNA:
control
Tom1L1
control
Tom1L1
wb: 4G10
-pY-CHC
wb: αCHC
ip:
αCHC
wb: αTom1L1.2
-Tom1L1
wb: αtubulin
-tubulin
WCL

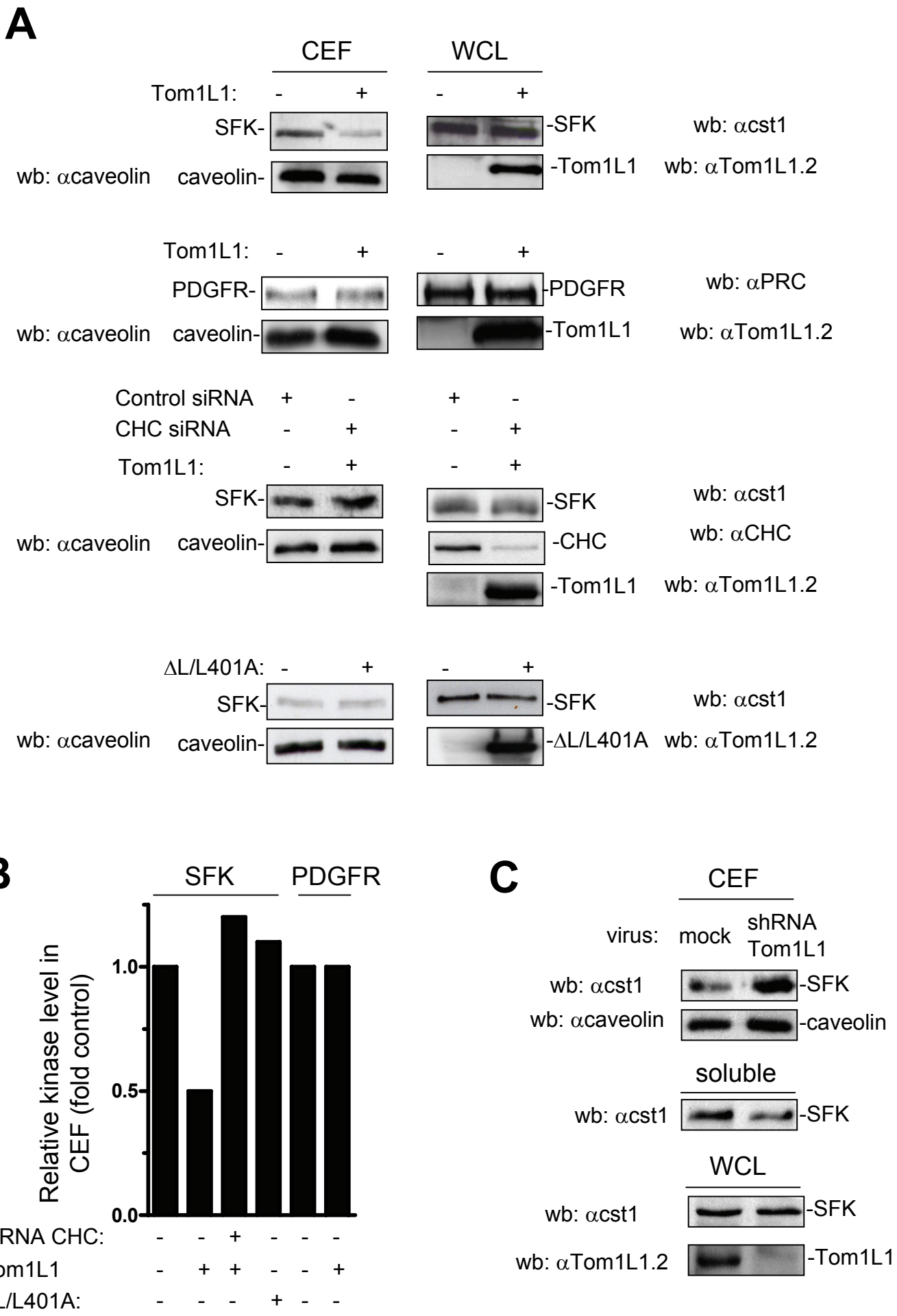
A
CEF
WCL
Tom1L1: - + - +
SFK-
-SFK
wb: αcst1
wb: αcaveolin
caveolin-
-Tom1L1
wb: αTom1L1.2
Tom1L1: - + - +
PDGFR-
-PDGFR
wb: αPRC
wb: αcaveolin
caveolin-
-Tom1L1
wb: αTom1L1.2
Control siRNA + - + -
CHC siRNA - + - +
Tom1L1: - + - +
SFK-
-SFK
wb: αcst1
wb: αcaveolin
caveolin-
-CHC
wb: αCHC
-Tom1L1
wb: αTom1L1.2
ΔL/L401A: - + - +
SFK-
-SFK
wb: αcst1
wb: αcaveolin
caveolin-
-ΔL/L401A
wb: αTom1L1.2
B
SFK
PDGFR
Relative kinase level in CEF (fold control)
1.0
0.5
0.0
siRNA CHC: - - + - - -
Tom1L1 - + + - - +
ΔL/L401A: - - - + - -
C
CEF
virus: mock shRNA Tom1L1
wb: αcst1
-SFK
wb: αcaveolin
-caveolin
soluble
wb: αcst1
-SFK
WCL
wb: αcst1
-SFK
wb: αTom1L1.2
-Tom1L1

D

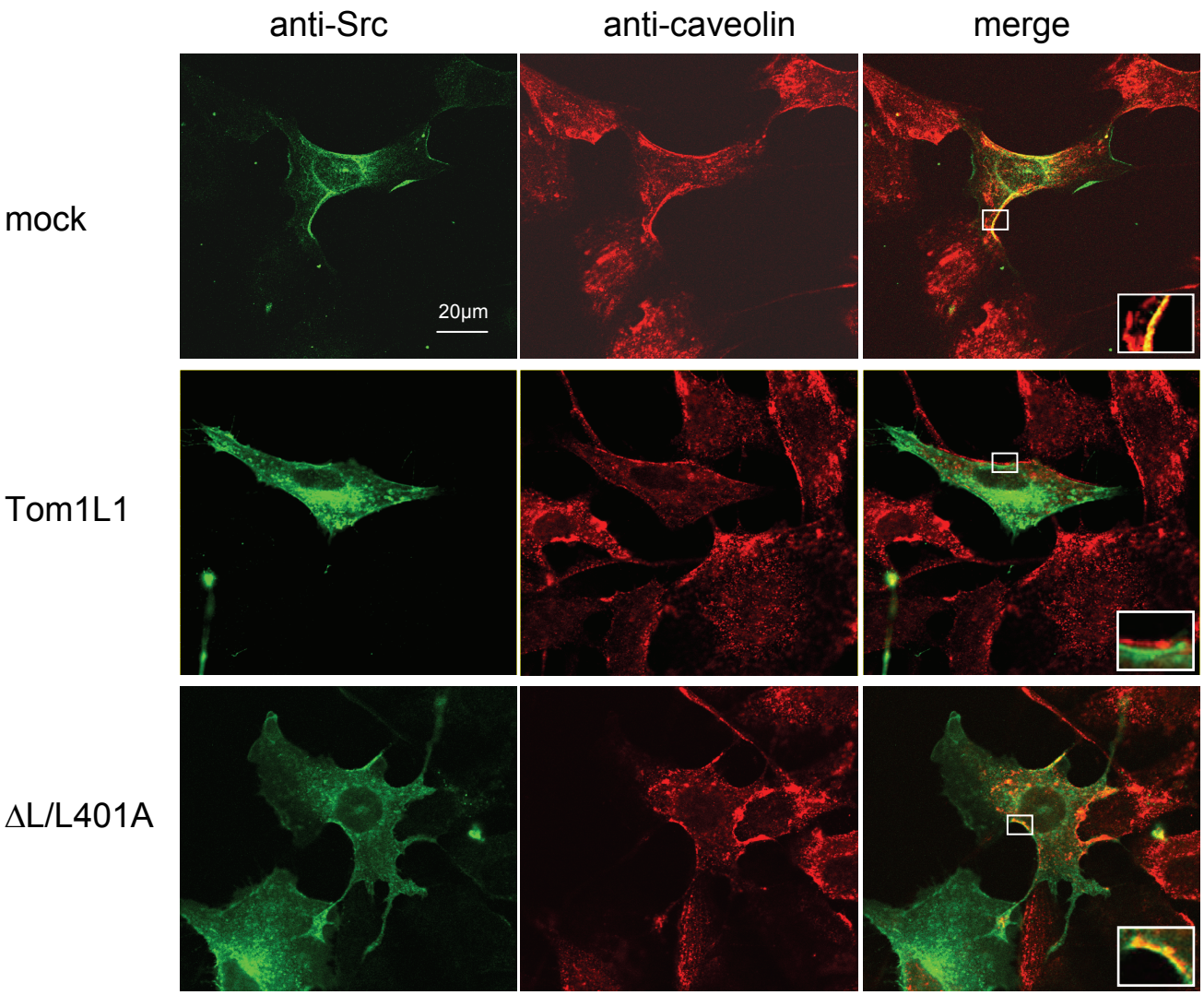
anti-Src
anti-caveolin
merge
mock
Tom1L1
ΔL/L401A
20μm

E

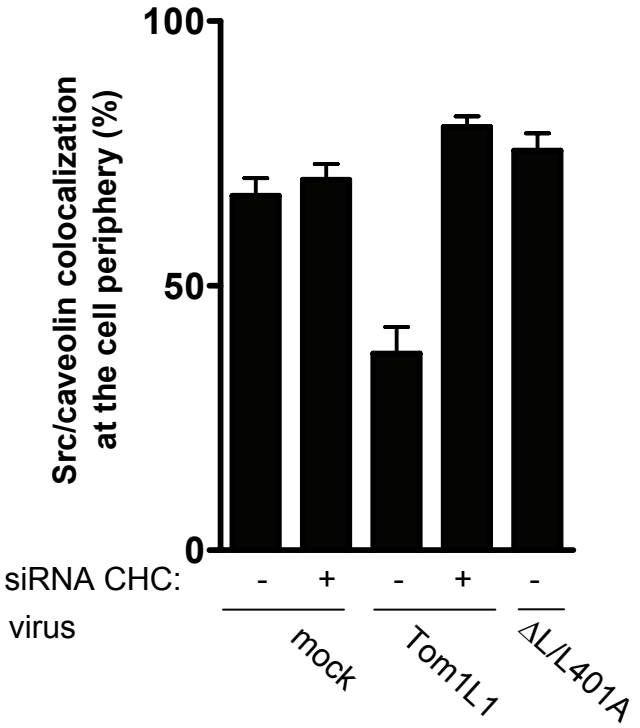
Src/caveolin colocalization at the cell periphery (%)
100
50
0
siRNA CHC:
- + - + -
virus
mock
Tom1L1
ΔL/L401A

Collin et al. Figure 5A, B

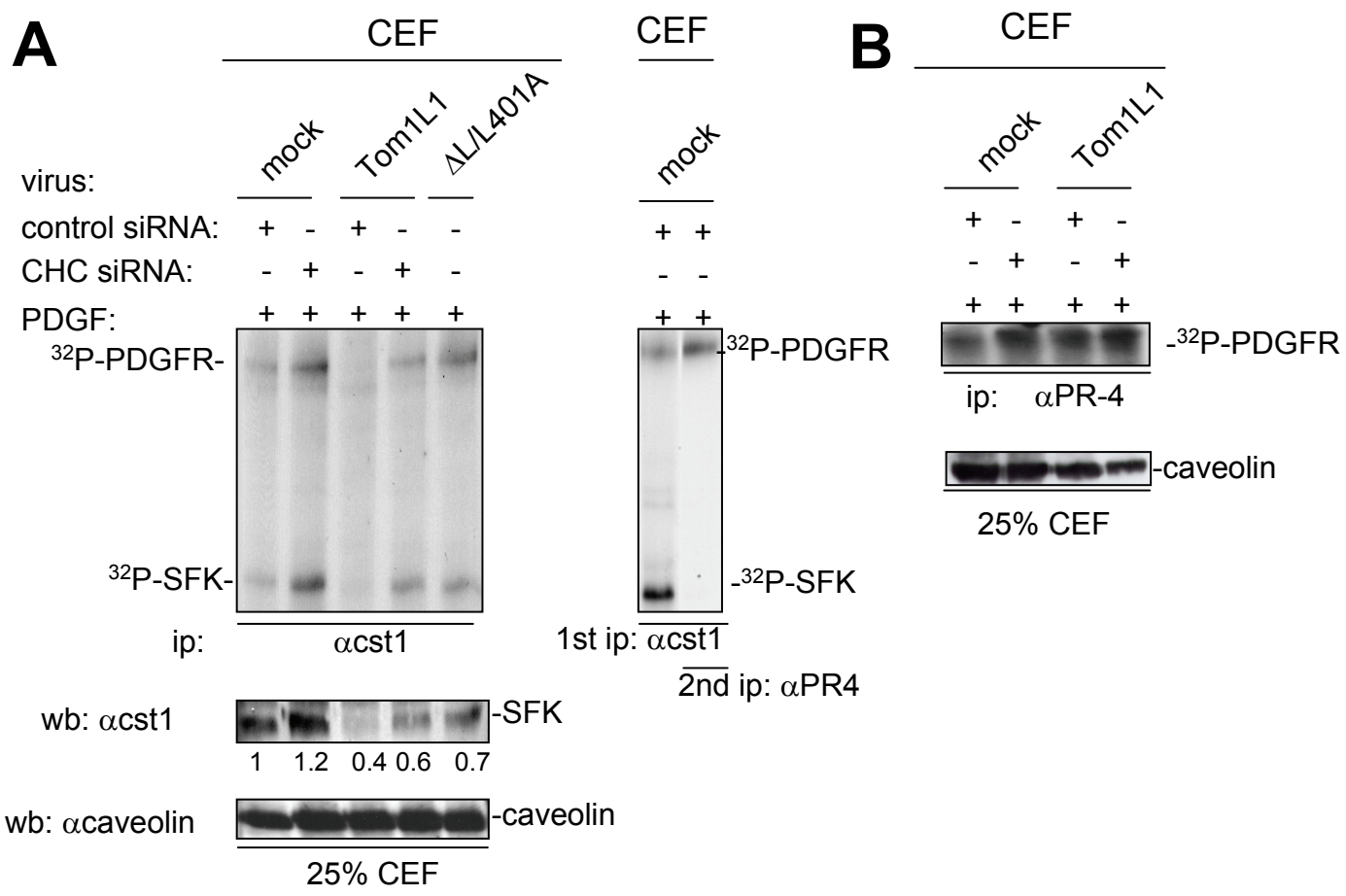

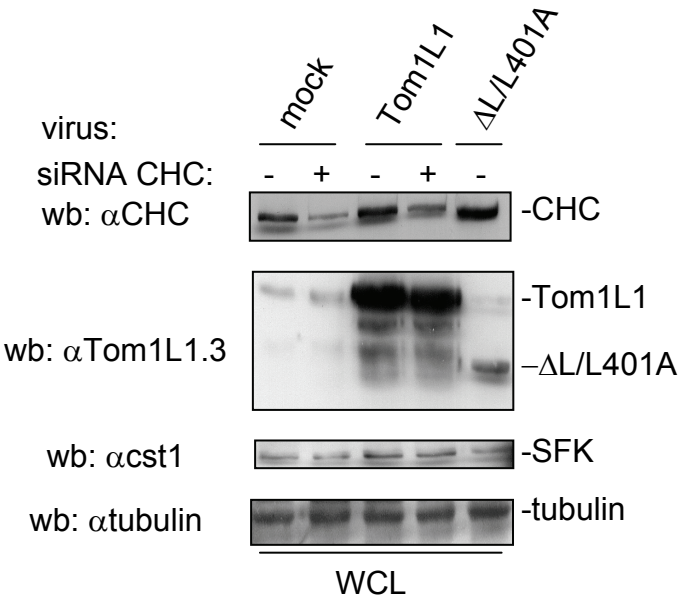

D

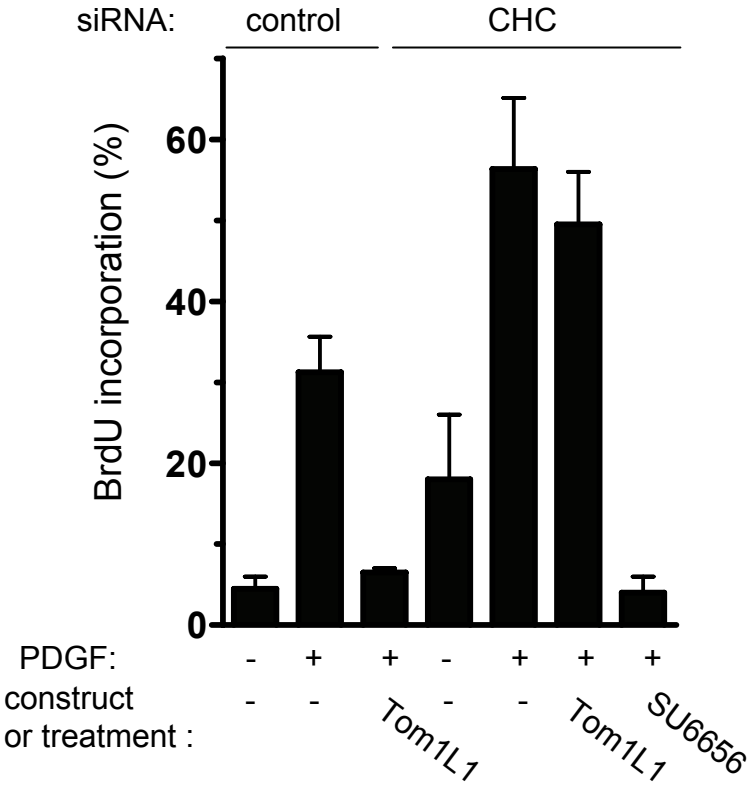
siRNA:
control
CHC
BrdU incorporation (%)
60
40
20
0
PDGF:
- + + - + + +
construct or treatment :
- - Tom1L1 - - Tom1L1 SU6656

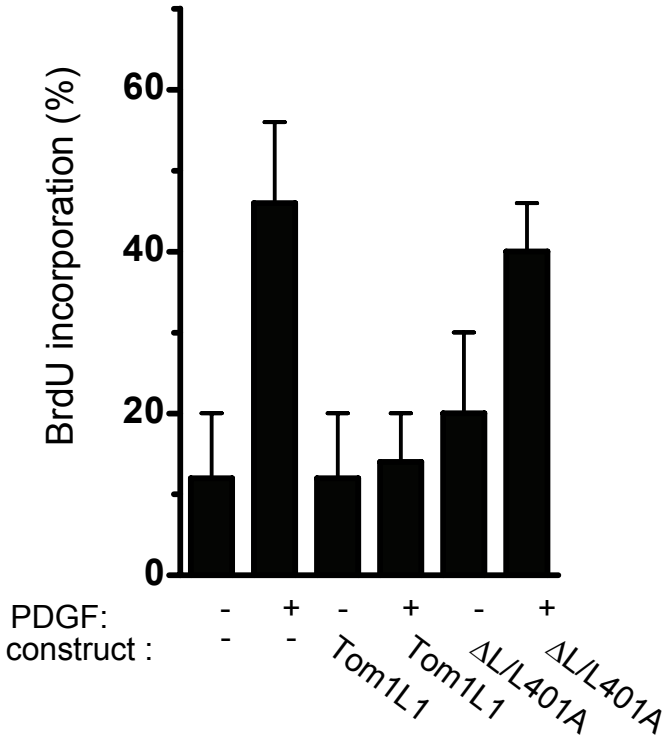
BrdU incorporation (%)
60
40
20
0
PDGF:
- + - + - +
construct :
- - Tom1L1 Tom1L1 ΔL/L401A ΔL/L401A

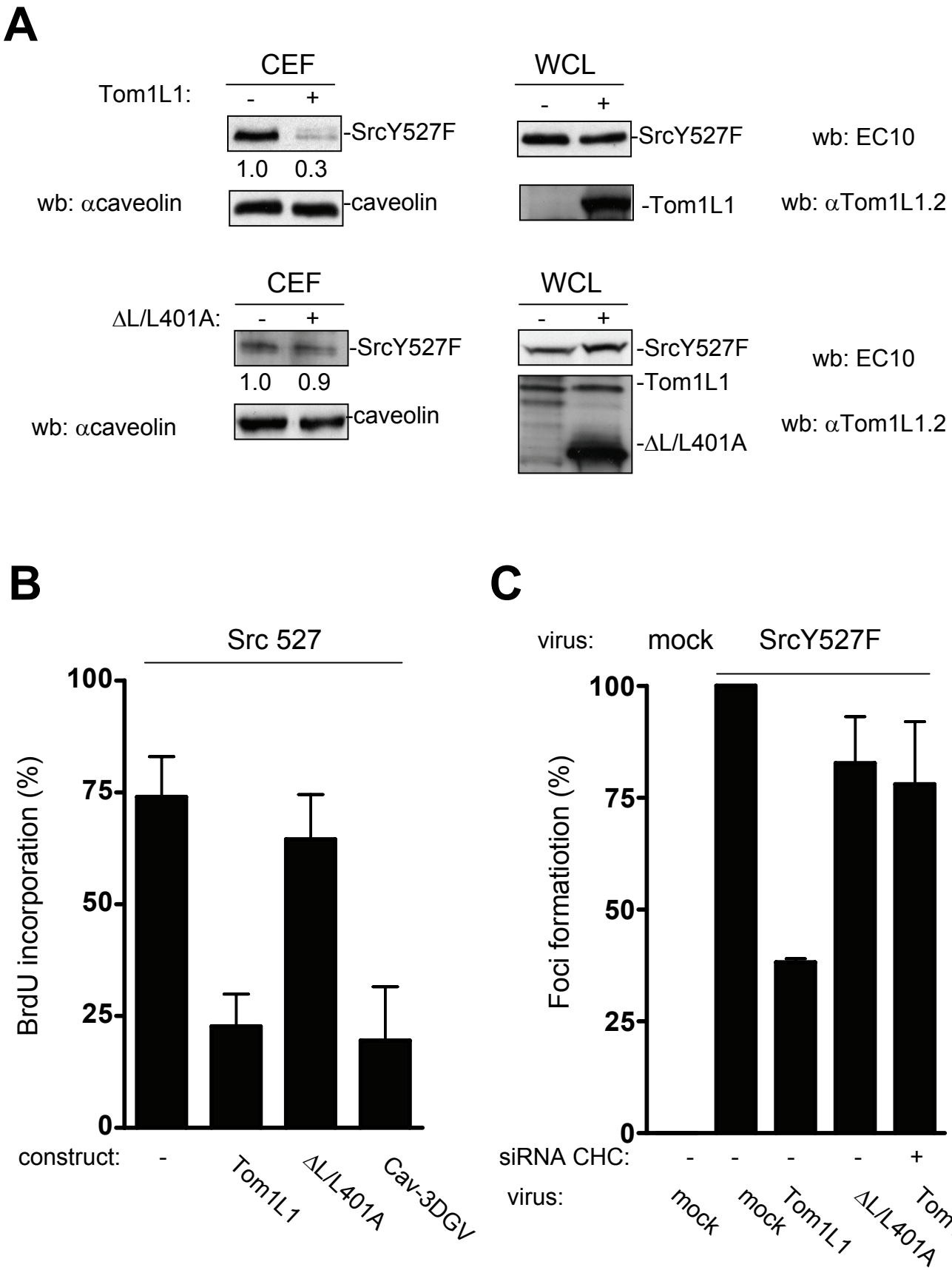
A
CEF
Tom1L1:
- +
-SrcY527F
1.0 0.3
wb: αcaveolin
-caveolin
WCL
- +
-SrcY527F
wb: EC10
-Tom1L1
wb: αTom1L1.2
CEF
ΔL/L401A:
- +
-SrcY527F
1.0 0.9
wb: αcaveolin
-caveolin
WCL
- +
-SrcY527F
wb: EC10
-Tom1L1
-ΔL/L401A
wb: αTom1L1.2
B
Src 527
BrdU incorporation (%)
100
75
50
25
0
construct: - Tom1L1 ΔL/L401A Cav-3DGV
C
virus: mock SrcY527F
Foci formatiotion (%)
100
75
50
25
0
siRNA CHC: - - - - +
virus: mock mock Tom1L1 ΔL/L401A Tom1L1

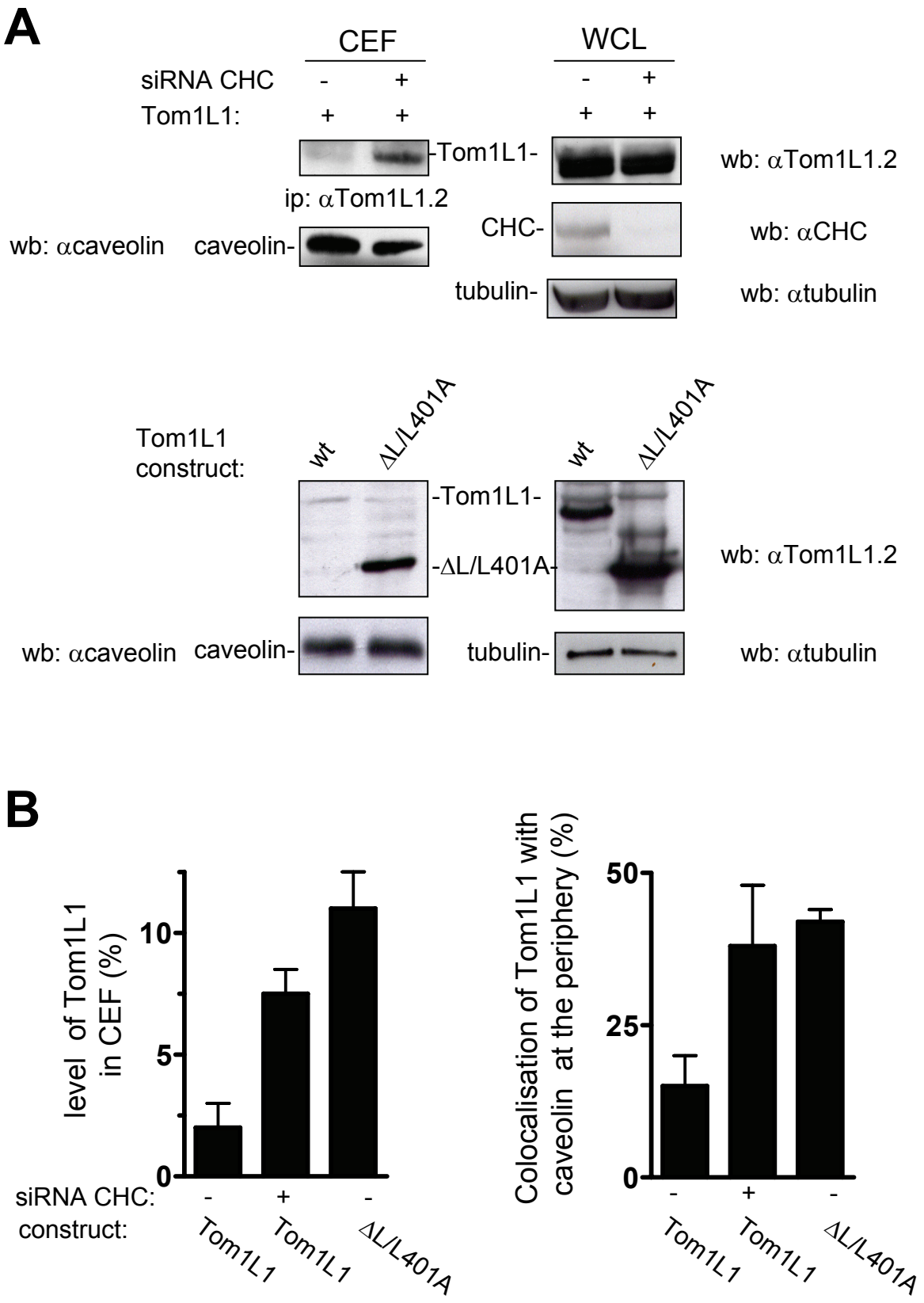
A
CEF
WCL
siRNA CHC - + - +
Tom1L1: + + + +
-Tom1L1-
wb: αTom1L1.2
ip: αTom1L1.2
wb: αcaveolin
caveolin-
CHC-
wb: αCHC
tubulin-
wb: αtubulin
Tom1L1 construct:
wt
ΔL/L401A
wt
ΔL/L401A
-Tom1L1-
-ΔL/L401A-
wb: αTom1L1.2
wb: αcaveolin
caveolin-
tubulin-
wb: αtubulin
B
level of Tom1L1 in CEF (%)
10
5
0
siRNA CHC: - + -
construct: Tom1L1 Tom1L1 ΔL/L401A
Colocalisation of Tom1L1 with caveolin at the periphery (%)
50
25
0
- + -
Tom1L1 Tom1L1 ΔL/L401A

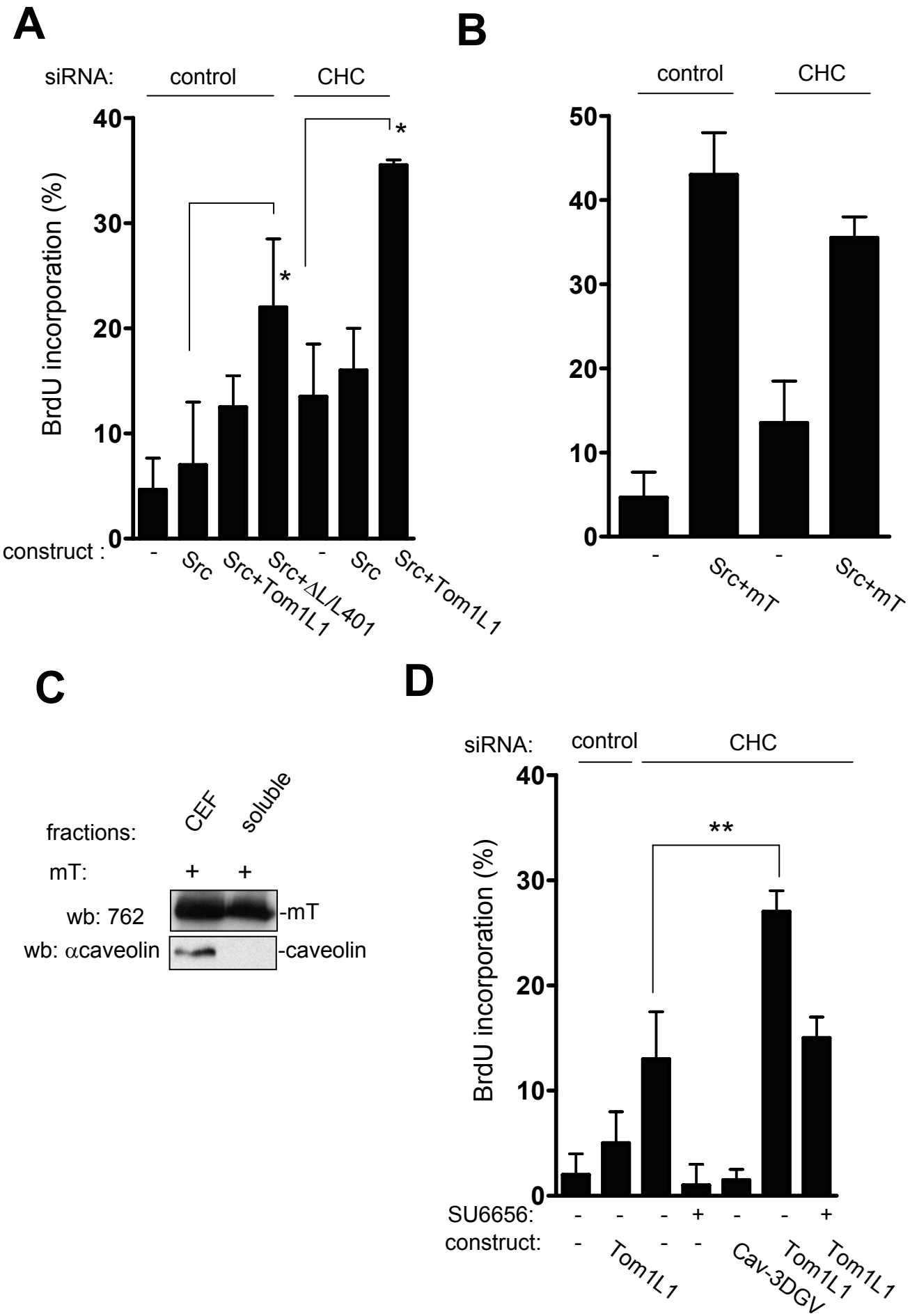
A
siRNA:
control
CHC
BrdU incorporation (%)
40
30
20
10
0
*
*
construct :
-
Src
Src+Tom1L1
Src+ΔL/L401
-
Src
Src+Tom1L1
B
control
CHC
50
40
30
20
10
0
-
Src+mT
-
Src+mT
C
fractions:
CEF
soluble
mT:
+
+
wb: 762
-mT
wb: αcaveolin
-caveolin
D
siRNA:
control
CHC
BrdU incorporation (%)
40
30
20
10
0
**
SU6656:
-
-
-
+
-
-
+
construct:
-
Tom1L1
-
-
Cav-3DGV
Tom1L1
Tom1L1